University of Essex - School of Computer Science and Electronic Engineering

PASSIVE IoT DEVICE WORKS WITH ENERGY HARVESTING

[Passive Watch Can Warn Blind People Of Nearby Vehicles Or Pedestrians By Vibration]

CE301 - Individual Capstone Project Challenge

BSc in Electronic System Engineering

Supervisor: *Hossein Anisi*

Second Assessor: *Jon Chamberlain*

Author: *Yu Wenlu*

1909135

wy19403@essex.ac.uk

Word Count: *12534*

Acknowledgements

I would like to express our sincere gratitude to everyone who contributed to the completion of this project. I have learned a lot during this process and could not have accomplished this without the help and support of many individuals and organizations.

First and foremost, I would like to thank our project supervisor Hossein Anisi, who provided me with invaluable guidance, support, and feedback throughout the project. His expertise and insight helped me to stay focused and motivated throughout the project. I would like to thank him for enhancing my personal academic skills. When I first entered my final semester, I was still confused and not very confident in my abilities. However, Professor Hossein always encouraged me, helped me to find my academic direction and guided me to learn and master the relevant knowledge and skills. Under his guidance, I began to familiarize myself with risk management, academic research processes and methods, and continued to improve my research skills and the various skills required. Throughout this process, Hossein has always provided me with the most professional guidance and assistance to successfully complete the ces301 challenge. In addition to this, I would like to thank him for his attention and assistance in my career development; Professor Hossein has not only guided and helped me in my academic research, but also in my career development and future, giving me very practical advice and guidance; Hossein has guided me in my future direction and prospects, giving me more and more confidence and confidence in my career path. His support and encouragement has given me the confidence that I will be able to achieve more in my academic research and career development. I would also like to thank Mohan Vishwanathan and the School of Computer Science and Electronic Engineering for providing me with the opportunity to undertake this project and for their continuous support and encouragement.

In the writing of this paper, I would like to give special thanks to my boyfriend whose teaching and help with my circuit diagram wiring and soldering skills was key to completing this research. I had gotten into trouble because I was unfamiliar with circuit diagram wiring and soldering skills, but my boyfriend was always there to help me. He has an in-depth knowledge and experience of these skills, and he has always been patient in guiding me and helping me with my problems. His expertise and experience have helped me immensely with my research. In addition to this, my boyfriend has provided a

lot of extra support and encouragement. He keeps me motivated by giving me moral support and encouragement when I need it.

Finally, I would like to thank my family for their unwavering support and encouragement throughout the project. Their love and support have been a constant source of strength and motivation throughout our journey. I would like to thank everyone who has contributed to this project, and I hope that my work will contribute to improving the lives of the visually impaired.

Abstract

Blind people face many challenges and risks when traveling in urban environments, especially when crossing roads or walking on sidewalks. They need a reliable and convenient device that can help them avoid collisions with vehicles and pedestrians. This project aims to design a passive watch that can warn blind people of nearby vehicles and pedestrians by vibration. The watch has several advantages over existing solutions, such as canes, guide dogs or smartphone apps, which are either cumbersome, expensive or require active operation. The watch is powered by a solar panel and uses an Arduino ultra-low power processor as the main control chip, which enhances its energy efficiency and durability. The watch employs millimeter wave radar technology to detect vehicles and personnel sensing radar technology to detect pedestrians, achieving comprehensive safety monitoring. The watch has two modes: optional mode and charge mode. In optional mode, the watch vibrates when vehicles and pedestrians are detected approaching from behind or the opposite direction within a certain distance. In charging mode, the watch switches off all sensors to save power and focuses on collecting energy with the solar panel and storing it. Users can switch between the two modes by lifting the solar panel pad. When the watch senses vehicles or pedestrians approaching, it vibrates to alert blind people. The vibration intensity and frequency vary according to the distance and speed of the approaching objects, providing more information for blind people to make decisions. The novelty of this design lies in integrating various technologies harmoniously, creating a product that has multiple functions, easy operation, low power consumption and environmental protection, meeting the needs of blind people's travel safety. The project also considers the user's comfort and aesthetics by designing a lightweight and stylish watch that can be worn on any wrist size.

Key Word

Passive

Embed system.

Millimeter Wave Radar

Wearable devices

Solar Panel

Io-T

Table of Contents

List of Symbols

1 **Thermoelectric generator (TEG)**: A TEG device is a thermoelectric generator that can convert heat into electricity by using the Seebeck effect. A TEG device consists of several thermocouples connected in series, where each thermocouple is made of two different materials with different Seebeck coefficients. The thermocouples are arranged so that one junction is exposed to a heat source and the other junction is exposed to a heat sink, creating a temperature difference across the device. The electric current generated by the Seebeck effect flows through the thermocouples and can be used to power an external load. A TEG device can be used for various applications such as waste heat recovery, energy harvesting, and cooling [1].

2 **Seebeck effect:** The Seebeck effect is a phenomenon that occurs when a temperature gradient is formed between two different conducting materials or a loop of one material, resulting in a voltage difference and an electric current. It was discovered by German physicist Thomas Johann Seebeck in 1821. The Seebeck effect can be used to measure temperature, generate electric power, or identify the composition of alloys. [1]

3 **P-type semiconductors:** Semiconductors that contain impurity atoms with one electron fewer than the host atoms, creating positive holes that can conduct current.

N-type semiconductors: Semiconductors that contain impurity atoms with one electron more than the host atoms, creating excess electrons that can conduct current [2].

4 **Polydimethylsiloxane (PDMS):** A type of silicone polymer that is widely used in biomedical applications, microfluidics, and soft lithography due to its biocompatibility, optical transparency, and low cost. PDMS is made by hydrolyzing dimethyldichlorosilane, which is produced from high-purity silica and methylene chloride by the Muller–Rochow reaction. The hydrolysis reaction produces hydrochloric acid and a polymer with silanol groups at the ends. These groups are then capped by reaction with trimethylsilyl chloride. The molecular weight and branching of PDMS can be controlled by using different silane precursors. [3].

5 **Conductive substrate:** A material that can support electric current flow and is used as a base for electronic devices or circuits. Examples of conductive substrates include metals, carbon nanotubes, graphene, and conductive polymers [3].

6 **Arduino Rev3 pinout** : The Arduino Rev3 pinout is the pinout on the development board that determines which external devices and sensors can be connected to the board [4]. Different boards have different pinouts, for example the FRDM-k32l2b board [5] used in development version A. The purpose of adapting the Arduino Rev3 pinout is to allow the board to be compatible with a wider range of expansion boards and modules, increasing the flexibility and convenience of development. The advantage of adapting the Arduino Rev3 pinout is that you can use the official Arduino documentation to learn quickly.

7 **FRDM k32L2B development board:** The FRDM k32L2B development board is a microcontroller development board manufactured by NXP Semiconductors [5]. It is designed for developing and testing applications based on the Arm Cortex-M0+ processor.

8 **MPPT:** MPPT stands for Maximum Power Point Tracking. It is a technique used with variable power sources, such as solar panels, to optimize the match between the solar array and the battery bank or utility grid. It converts a higher voltage DC output from solar panels down to the lower voltage needed to charge batteries. It also adjusts the load characteristic as the conditions change, such as sunlight intensity and temperature, to extract the maximum power from the solar panels [6].

Chapter1. Introduction

Blind individuals face numerous challenges and risks when traveling in urban environments, particularly when crossing roads or walking on sidewalks. They require a reliable and convenient device to help them avoid collisions with vehicles and pedestrians. This project aims to design a passive watch that can alert blind individuals of nearby vehicles and pedestrians through vibration. The watch has several advantages over existing solutions such as canes, guide dogs, or smartphone apps, which are either cumbersome, expensive, or require active operation.

The proposed watch is powered by a solar panel and utilizes an ultra-low power Arduino processor as the main control chip, enhancing its energy efficiency and durability. The watch employs millimeter wave radar technology to detect vehicles and personnel sensing radar technology to detect pedestrians, providing comprehensive safety monitoring. The watch has two modes: optional mode and charge mode. In optional mode, the watch vibrates when it detects vehicles or pedestrians approaching from behind or in the opposite direction within a certain distance. In charging mode, the watch turns off all sensors to save power and focuses on collecting energy with the solar panel and storing it. Users can switch between the two modes by lifting the solar panel pad.

When the watch detects vehicles or pedestrians approaching, it vibrates to alert the blind individual. The vibration intensity and frequency vary according to the distance and speed of the approaching objects, providing more information for blind individuals to make informed decisions. The novelty of this design lies in the harmonious integration of various technologies, resulting in a product that has multiple functions, easy operation, low power consumption, and environmental protection, meeting the travel safety needs of blind individuals. Additionally, the project considers user comfort and aesthetics by designing a lightweight and stylish watch that can be worn on any wrist size. The proposed passive watch has significant potential to enhance the safety of blind individuals in urban environments. The integration of various technologies, the utilization of renewable energy, and the emphasis on user comfort and aesthetics demonstrate the watch's suitability as a practical and sustainable solution to address the challenges faced by blind individuals.

Chapter2. Literature Review

Blind and visually impaired people often face difficulties in navigating busy urban streets, especially when it comes to crossing roads. With the advancement of technology, smart wearable devices have emerged as a potential solution to help these individuals navigate roads safely.

Inclusive City Maker's article describes the challenges and skills involved in crossing roads for blind and visually impaired people [7]. The article discusses how tactile paving, acoustic traffic signals, and smartphone apps can assist these individuals. Tactile paving, also known as tactile ground surface indicators, provides tactile cues to guide people to the crossing. Acoustic traffic signals emit audible signals indicating when it is safe to cross. Smartphone apps can provide audio instructions and real-time information about traffic patterns, helping the user to safely navigate their surroundings. Leonardi et al.'s paper [8] discusses the use of flexible solar panels to power a blood oxygenation sensor and a Bluetooth module in a smart bracelet. This technology has the potential to assist blind individuals in crossing roads by providing real-time feedback on traffic patterns and traffic light changes.

The use of millimeter wave radar technology in wearable devices is a promising area of research due to its ability to provide high-resolution sensing and tracking capabilities. Some research discusses the principles and advantages of millimeter Wave radar technology and its integration into various applications, including wearable devices. On the other hand, self-powered wearable systems have also garnered attention due to their potential for long-term and autonomous operation [9]. Some research different types of energy harvesting technologies for portable and wearable devices are reviewed, including mechanical, thermal, chemical, and solar energy. This review article also presents examples of self-powered systems with sensing, actuation, and intelligent functions [10]. Moreover, the feasibility and efficiency of solar energy harvesting for wearable healthcare applications are demonstrate [8]. This paper presents the design and implementation of a smart bracelet that uses flexible solar panels to power a blood oxygenation sensor and a Bluetooth module. These three papers collectively provide insights into the principles, advantages, and applications of millimeter Wave radar technology and energy harvesting technologies for wearable devices.

The Sunu Band is a smartwatch designed to assist blind individuals in navigating their surroundings. It uses sonar and echolocation to detect objects within a range of up to 16 feet and provides haptic feedback to the wearer. According to Gus Alexiou in Forbes, the device has proven useful in helping blind people maintain social distance during the pandemic. [11] Rachel Metz from MIT Technology Review explains that the Sunu Band can help visually impaired individuals avoid obstacles, find doorways, and sense traffic lights. [12] In addition to the Sunu Band, various technologies have emerged to aid blind people in crossing the road safely. Tactile paving and acoustic traffic signals are examples of external cues that provide information on crossing directions and traffic flow. Guide dogs can also provide visual cues and navigation assistance to blind individuals. According to WebMD, the use of external cues in combination with proper training and orientation can help blind pedestrians navigate busy streets safely. [7]

Chapter3. Methodology

This chapter explains the methods and techniques used for data collection, analysis, and interpretation in this research, such as millimeter-wave radar, time-of-flight sensors, and vibration motors. It also describes the steps followed to address ethical considerations in the research process. Moreover, the chapter identifies the limitations of the chosen approach and the actions taken to reduce their effects. The ethical issues and limitations are further discussed in detail. By presenting the methodology, the reader can understand the quality and validity of the research, and evaluate the trustworthiness of the findings reported in the document.

1 Module Test

This section presents some of the preliminary work that has been done to complete the project. One of the main tasks was to develop a flexible thermoelectric generator (TEG) that can harvest body heat and convert it into electrical energy. A flexible TEG is a desirable device for wearable applications and internet of things (IoT) sensors, as it can conform to complex shapes and provide a continuous power supply. However, making a flexible TEG is challenging due to the trade-off between flexibility and performance. I attempted to make a flexible TEG by disassembling a rigid TEG and replacing the hard shell with a soft material. However, this resulted in a lower output voltage and power than the original TEG, and the device was still not flexible enough. Therefore, I abandoned this idea and decided to connect multiple small TEGs in series to increase the power output. Another task was to test different types and sizes of solar panels that can convert light into electricity. Solar panels are another potential source of energy for wearable devices and IoT sensors, as they can harvest ambient light and provide a stable voltage output . I tested seven solar panels with varying materials and dimensions. I found that the flexible solar panels had a higher power output but a lower voltage output than the rigid solar panels. However, they were also less efficient and more expensive than the rigid solar panels.

1.1 Source 1 Thermoelectric Generator (TEG)

This section reports some of the preliminary work that has been done to complete the project. One of the main objectives was to develop a flexible thermoelectric generator (TEG) that can harvest body heat and convert it into electrical energy for wearable and IoT applications . Flexible TEGs are devices that can convert waste heat into electricity

by using thermoelectric materials that are flexible and wearable. Flexible TEGs have potential applications in powering sensors, lighting LEDs, and monitoring biomechanical motions. A flexible TEG is desirable because it can conform to complex shapes and provide a continuous power supply.

However, making a flexible TEG is challenging due to the trade-off between flexibility and performance, as well as the difficulty of finding suitable materials and fabrication methods. I searched online for different types of TEGs, but none of them met my requirements. They were either too rigid, too large, or too expensive. According to one review article [13], flexible TEGs can be classified into three categories based on the type of thermoelectric materials: flexible substrate supported films, organic-chalcogenide composites, and free-standing flexible films. Each category has its own advantages and disadvantages in terms of power factor, figure of merit, flexibility, and stability. I also emailed the author of a paper that described a flexible TEG, but I did not get a reply.

My motivation for this project was to overcome the limitations of the current TEGs and create a novel flexible TEG that can achieve high output power and voltage, low production cost, and good flexibility. To achieve this goal, I tried two different approaches. The first approach was inspired by a video on YouTube that showed how to make a TEG from scratch using P-type and N-type semiconductor [14]. However, I realized that soldering 10,000 semiconductors by hand was too difficult and time-consuming. The second approach was based on some papers that explained how to make flexible TEGs by disassembling rigid TEGs and replacing the hard shell with a soft material [15] [16]. I followed the steps in these papers and attempted to make a flexible TEG using PDMS as a conductive substrate, as shown in Figure 1.

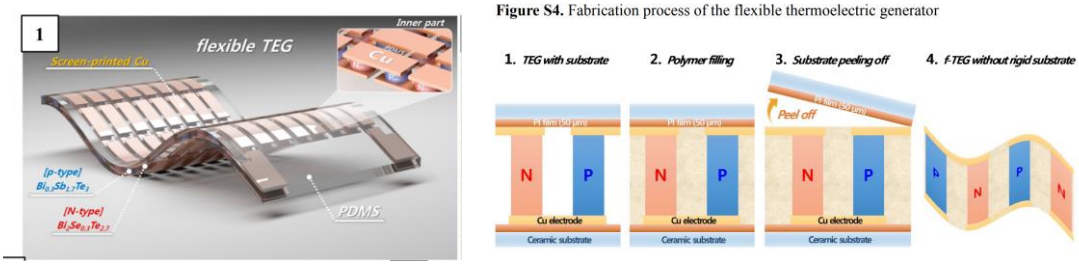

Figure 1 Previous Research Used PDMS To Make Flex TEG [15] [16].

However, both approaches failed to produce satisfactory results. I encountered several problems during the fabrication process, such as low output voltage and power, poor

flexibility, and high production cost (Figure 2). Therefore, I abandoned these ideas and decided to explore other possible solutions.

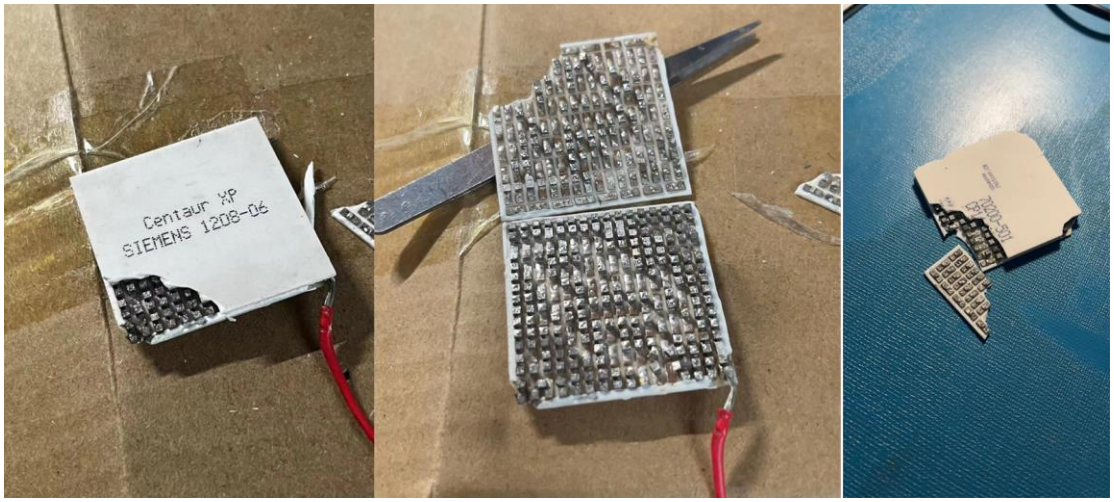

Figure 2 Thermoelectric Sheet Test Process.

I then turned to small TEGs measuring 6mm x 6mm x 3mm, which were more readily available and affordable. I connected multiple small TEGs in series and achieved moderate success, with an output voltage of 5mV and a power output of 0.1mW.

1.2 Source 2 Solar Panel

In this section, I will discuss the existing and related works that led to my motivation and objectives for this project. The primary objective was to compare the performance of different solar panels suitable for wearable and IoT applications. Solar panels are a promising source of energy as they can harvest ambient light and provide a stable voltage output. However, selecting the right solar panel involves a trade-off between size, efficiency, cost, and flexibility. I reviewed the existing literature on different types of solar panels, but none of them met my requirements. This led me to test seven solar panels with varying sizes and materials, including five flexible and two rigid ones.

My motivation for this project was to find a solar panel that could achieve high output power and voltage, low cost, and good flexibility. To accomplish this goal, I conducted a comprehensive comparison of the seven solar panels' performance based on

Table 3, which provided a quantitative analysis of the open circuit voltage, maximum power point voltage, maximum power point current, and maximum power point power of each solar panel.

The results showed that the flexible solar panels had an average output of 7.7 volts,

indicating that each solar panel could generate approximately 1.5 volts. To evaluate the flexibility of the solar panels, I conducted experiments on their bending properties by folding them at different angles and measuring their voltage output. The results indicated that the voltage output of the flexible solar panels was not significantly affected by folding, as shown in Figure 3.

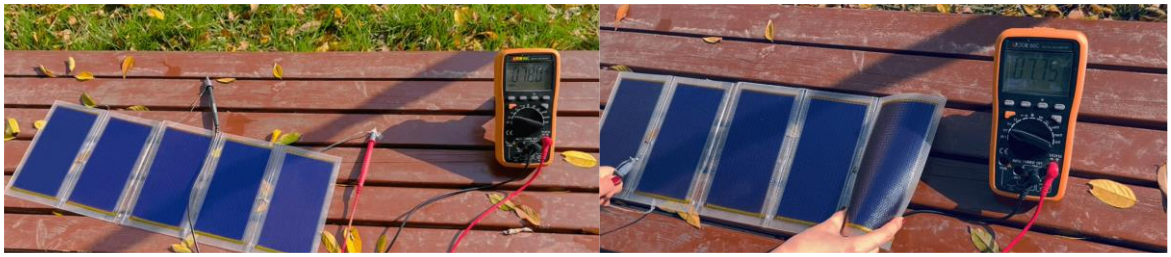

Figure 3 Flex Solar Panel Testing Process

However, the rigid solar panels had some trade-offs in terms of comfort. They were able to produce ten times more power than the flexible solar panels under the same surface area. To test the flexible solar panels in action, I connected them to a monolith and a small screen of LEDs, as depicted in Figure 4. The experiment demonstrated that three flexible solar panels were enough to power one LED. However, decreasing the number of solar panels to two led to a noticeable dimming of the screen, and further reduction to one solar panel caused the LEDs to turn off completely, especially in the later part of the day when the sun intensity is low.

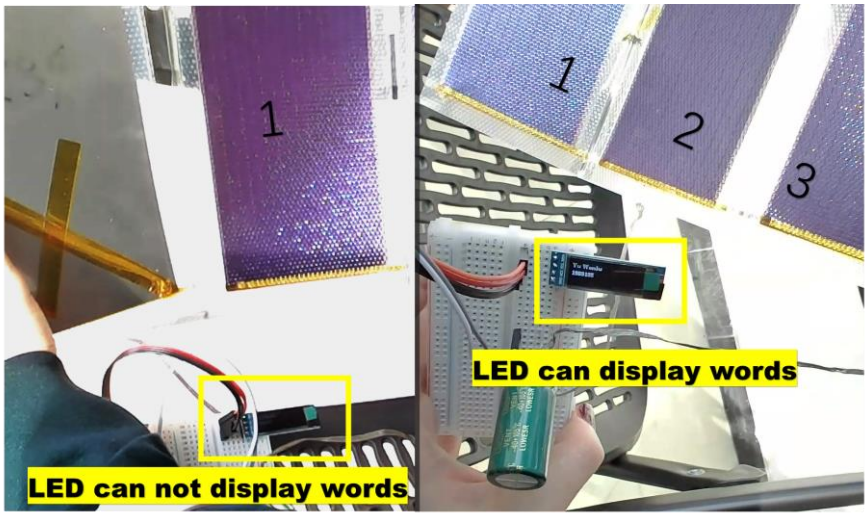

Figure 4 Comparing the power of solar panels of different sizes.

To address this challenge, I realized that future designs would need to incorporate batteries or capacitors to store energy. Moreover, the entire project would require battery management and boost chips to regulate the power supply of the system.

In this module, we have tested several energy harvesting systems from different sources, of which the flexible energy harvesting system in particular was analyzed and studied in depth, but the results were not particularly satisfactory and, in summary, the flexible energy harvesting system probably has the following drawbacks:

- The trade-off between flexibility and efficiency, as increasing the flexibility may reduce the thermoelectric efficiency / light absorption or charge transport of the photovoltaic materials or vice versa.
- The challenge of maintaining good adhesion between the photovoltaic layers and the substrates / thermoelectric legs and the electrodes, especially under bending or stretching conditions.
- The degradation of photovoltaic/ thermoelectric properties due to oxidation, moisture, or mechanical fatigue.

2 Shield Board A

The proposed project idea is to design a shield that can harvest energy from the environment and use radar detection to warn blind people of nearby vehicles and pedestrians for a preview. The idea faces significant challenges due to the limited energy resources and the complex functionality involved. Therefore, energy management and provision had to be considered, as well as the choice of the main controller chip, to ensure the feasibility and functionality of the design. The motivation for this version of the shield board was to explore the potential for harmonious integration of various technologies to create a possible product with multiple functions, easy operation, low energy consumption and environmental friendliness. The objective of this section is to design, implement and evaluate a prototype shield board to demonstrate the feasibility and functionality of the proposed project idea.

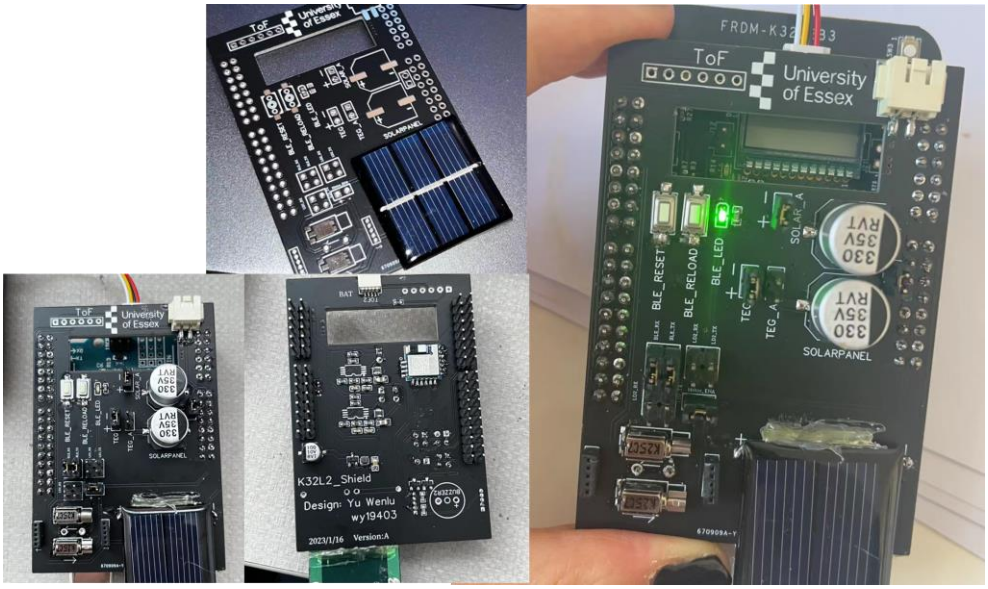

Figure 5 Shield Board A Physical Photos.

2.1 Describes the function and purpose of the board.

The first phase of this project involves designing a shield board that can be attached to a FRDM K32L2B development board and serve as a proof-of-concept prototype for the passive watch idea. The shield board integrates energy harvesting, vibration motors, serial communication and millimeter wave radar detection technologies, which are essential for the functionality of the passive watch. The shield board can also help to test the performance and compatibility of these technologies, as well as to identify and solve any potential problems or challenges that may arise in the implementation process. The motivation of this phase is to demonstrate the feasibility of the passive watch idea and to provide a basis for further development and improvement. The objectives of this phase are to design, implement and evaluate a shield board prototype that can meet the functional requirements and specifications of the passive watch idea.

2.2 Explain the main components and devices on the circuit board.

The shield board includes an energy harvesting circuit and a millimeter-wave radar detection circuit, and is connected to the FRDM K32L2B development board through the SPI interface. The shield circuit board is a two-layer PCB with a size of 50mm x 70mm as shown in Figure 6. It is made of FR4 material and has a ground plane on the bottom layer to reduce noise and improve signal integrity. The board has several components including resistors, capacitors, diodes and ICs.

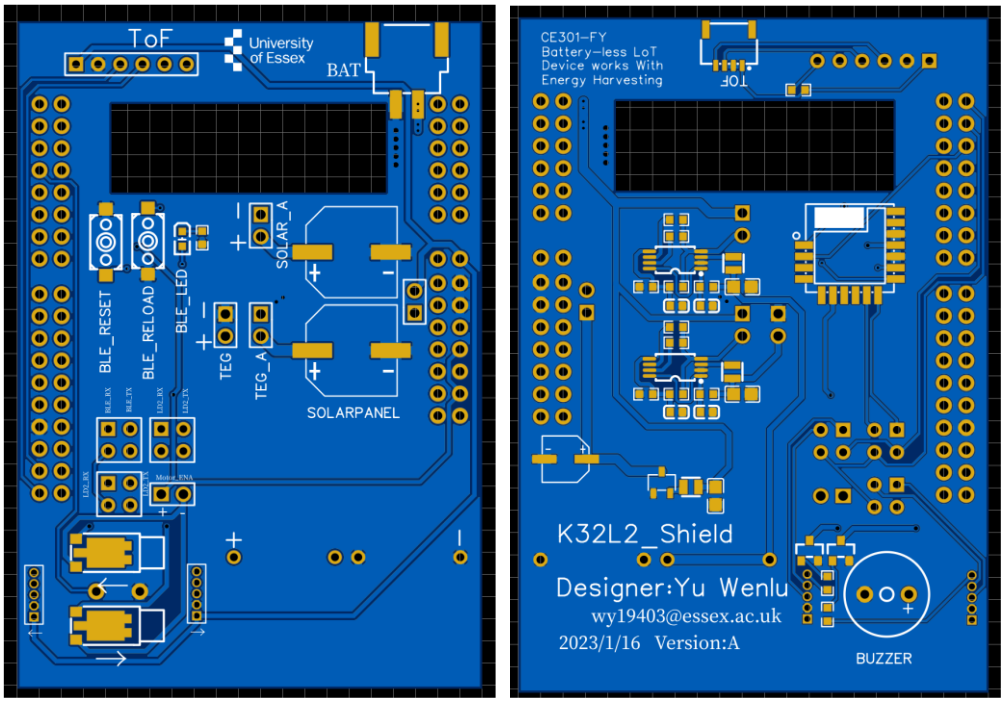

Figure 6 Shield Board A PCB 2D Photo.

For main components:

- **WH-BLE106 [Low power Bluetooth]**: A module that implements Bluetooth communication with low power consumption. It supports Bluetooth 5 features such as higher data throughput, longer range and increased broadcasting capacity [17].

- **LD2410[millimeter wave sensor]:** With its small size, low power consumption, high sensitivity, high cost performance and high performance, the LD2410 millimeter wave sensor is a 24G human presence sensing radar module that can detect human presence, micro-movement and motion within 6m. A module that controls two DC motors with PWM signals. It has a built-in H-bridge driver and can adjust the speed and direction of the motors. [18]

- **SPV1040TTR [Boost converters]**: low-power, low-voltage monolithic boost converter capable of maximising the energy generated by solar cells with strong low input voltage handling capabilities. It also has a built-in MPPT algorithm to provide the highest energy conversion efficiency under different environmental conditions. [19]

2.3 Analysis of the board's working principles and performance.

The shield prototype is designed to demonstrate the feasibility and functionality of the proposed project idea. It consists of several components and connectors that allow for operation under various conditions. The FRDM K32L2B development board serves as the primary controller and executes the firmware for the Passive Watch project.

One of the main features of the shield is the Time-of-Flight (ToF) module, which uses infrared light to measure distance and speed. The header H1 is connected to the ToF module, which can detect objects in front of the watch. Additionally, the WH-BLE106 module, U3, establishes a low-power Bluetooth communication link with the host PC, outputting debugging information.

Another important aspect of the shield is the energy harvesting system, which utilizes two SPV1040TTRs to boost the voltage output of the solar panel and TEG to 4.2V to charge the lithium-ion battery. The output voltage and maximum output current are regulated using an external resistor divider and sense resistor, providing efficient management of the power supply for the entire circuit. The proper and stable power supply of the development board is particularly important, as it is integral to the watch's functionality. Effective power management not only ensures optimal performance but also extends the battery life of the watch. The TEG/solar panels and the FRDM K32L2B development board, which serve as the energy sources for the watch, are connected to the J8, J1, and J2 pins, allowing for the measurement of maximum power output using an external ammeter and a duplex cable, utilizing Maximum Power Point Tracking (MPPT) of the SPV1040TTR chips.

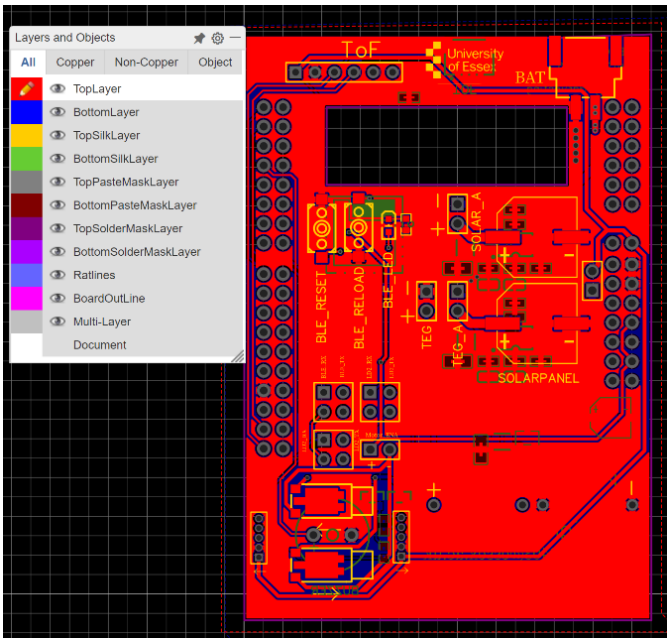

Figure 7 Shield Board A PCB layer.

The last component of the shield is the radar detection system, which uses LD2410 modules to generate and receive radar signals using microwave pulses. These radar signals can be selectively transmitted to the FRDM K32L2B development board for filtering or processing or to the host PC for analysis by shorting different pins in J3, J4, and J5 using jumper caps.

2.4 Advantages and disadvantages

– ***For energy harvesting:*** The circuit design for this board incorporates the SPV1040TTR chip to track the maximum power of the solar panel and TEG energy sources. However, the performance of the SPV1040TTR chip differs significantly between the two sources. For the solar panel, the SPV1040TTR chip can effectively track the maximum power output under varying sunlight conditions. For the TEG, however, the SPV1040TTR chip has a minimal impact on the power output. This is mainly due to the characteristics of the TEG, which generates a high instantaneous current when a hot object first contacts the thermoelectric sheet. However, because the board lacks adequate heat dissipation mechanisms, the high output current of the TEG only lasts for less than 9.2 seconds, and then drops significantly as the temperature difference decreases. Therefore, the SPV1040TTR chip cannot optimize the power output of the TEG over a longer period.

- ***Energy management and provision:*** One of the challenges of the shield board design is to ensure a stable and sufficient voltage input to the main controller chip FRDM K32L2B, which requires a minimum of 3.3V to operate. However, the solar panel and the TEG have limited energy harvesting capabilities due to their small size and low efficiency. Moreover, the energy output of these sources is highly dependent on the environmental conditions, such as sunlight intensity and temperature difference. Therefore, the shield board often fails to provide a constant voltage input to the FRDM K32L2B, resulting in intermittent or insufficient power supply for the development board and its functions.

- ***For the MCU:*** The initial choice of the main controller chip for the shield board was the K32L2 from NXP, which offered the advantages of low power consumption and high processing efficiency. However, during the firmware development process, several challenges were encountered with this chip. First, the chip was out of stock and difficult to purchase from the market, which limited the availability and scalability of the final design. Second, the chip was expensive compared to other alternatives, which increased the cost and reduced the affordability of the shield board. Third, the chip had complex functions that exceeded the requirements of the initial design, but the functions that were needed were simple and hard to debug. Fourth, the chip had limited online documentation and support, which made it difficult to find solutions when problems occurred.

- To improve the detection accuracy and reliability of the passive watch, ***the ld2410 millimeter wave radar module*** was chosen as the main sensor for human presence detection. This module can detect human presence within a range of 6 meters, regardless of environmental conditions such as light, temperature or humidity. However, a challenge encountered in this project was that the ld2410 module could not differentiate between the user (blind) and other pedestrians in the vicinity, especially when they were close to each other or moving in the same direction. This caused the ld2410 module to send a constant “human presence” signal to the MCU and motor, even when there was no pedestrian approaching from behind or from the opposite direction. As a result, the watch would vibrate continuously, confusing the user and disrupting the normal operation of the detection function.

3 Demo Board B

The main objective of this section is to design a passive watch that can integrate various technologies harmoniously, such as millimeter-wave radar, time-of-flight sensor, vibration motor, battery management chip and low-power Bluetooth module. The watch is powered by a solar panel that can be flipped open or closed to switch between charging mode and working mode. The watch also has a protective shell and hinges to enhance its durability and user-friendliness. The improvement of Demo Board B over Shield Board A is that it uses a more compact and integrated design that can fit on a wristband, rather than a separate shield board that needs to be attached to a development board. The watch also uses a more advanced battery management chip that can operate at 79 GHz, rather than 60 GHz, providing higher resolution and accuracy. The motivation for this version of the circuit is to build on the test results of the previous version of the shield board to provide a reliable and accessible device that can help blind people avoid collisions with vehicles and pedestrians, a common challenge and risk when they travel in urban environments. The novelty of this design lies in combining millimeter-wave radar technology with energy harvesting technology, creating a product that has multiple functions, easy operation, low power consumption and environmental protection, meeting the needs of blind people's travel safety. The project also considers the user's comfort and aesthetics by designing a lightweight and stylish watch that can be worn on any wrist size.

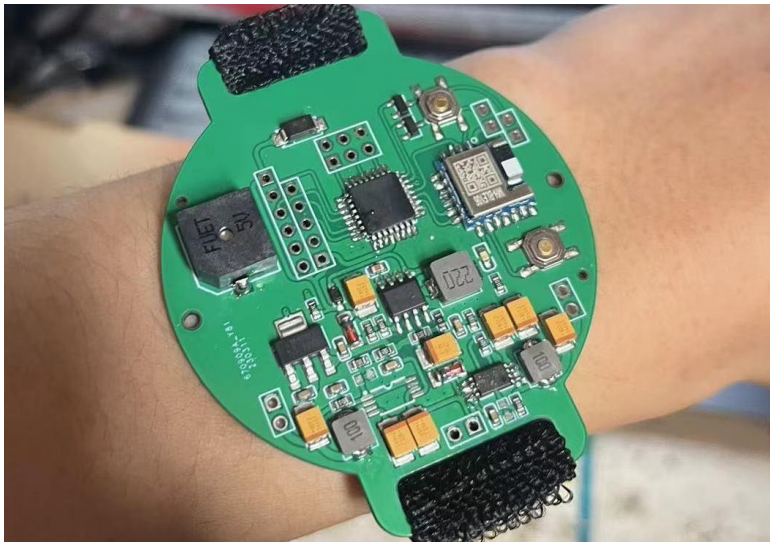

Figure 8 Demo Board B PCB sample

3.1 Describes the function and purpose of the board.

Demo Board B is a solar-powered watch that uses millimeter-wave radar to detect the direction of pedestrians and alerts the user through a vibration motor. It is an improved

version of a previous circuit board design, with added features such as a protective shell, hinges, and the ability to choose the charging mode and working mode. The new millimeter-wave radar technology allows for accurate detection of pedestrians, and the vibration motor alerts the user without the need for visual cues. The protective 3D print shell and added mechanical parts make the device more durable and user-friendly, while the ability to choose charging and working modes adds flexibility to the device.The objectives of this design are to provide a reliable, convenient and non-intrusive device that can help blind people avoid collisions with vehicles and pedestrians by using advanced radar technology and haptic feedback. In the following sections, I will discuss their advantages and disadvantages, and explain the main components and devices on my circuit board.

3.2 Explain the main components and devices on the circuit board.

The circuit board in question contains several sensor modules, including a ToF sensor, a millimeter-wave radar detection module, a buzzer, and two vibrators. Additionally, the board includes a battery management chip and an Atmega328P chip for signal processing and control logic. The board can operate in two different modes, depending on the state of a switch.

- **Atmega328P [MCU]:**The Atmega328P is a microcontroller chip from the Atmel AVR family, which is widely used in various electronic devices and projects. It has 32KB of flash memory, 2KB of SRAM, and 1KB of EEPROM memory. The Atmega328P has 23 input/output pins, including 6 analog input pins, and can operate at a maximum frequency of 20MHz. The Atmega328P features multiple communication interfaces, including two USARTs, an SP, and an I2C interface. It also has a 10-bit analog-to-digital converter (ADC) with up to 8 channels and a programmable gain amplifier.

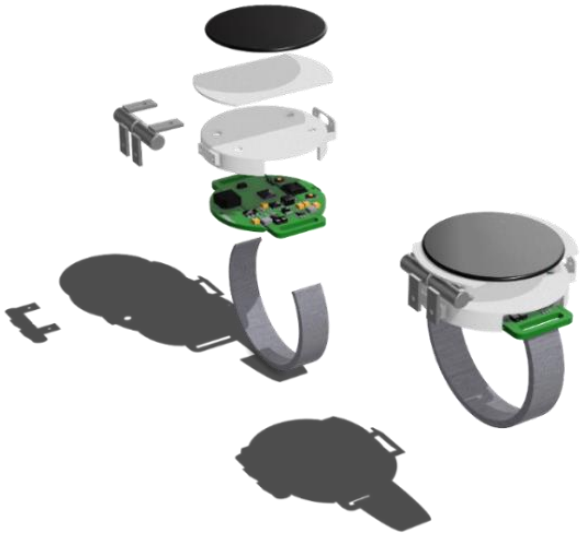

Figure 9 Demo Board B 3D Rendering model

– **LD7903A [millimeter-wave high-frequency radar]:**The LD7903A is a highly advanced millimeter-wave high-frequency radar sensing module, designed for presence detection and trajectory tracking of human bodies in indoor environments. It operates at a frequency of 79 GHz and uses frequency modulation continuous wave (FMCW) technology to accurately detect human presence and movement. The module has a small form factor and low power consumption, making it ideal for integration into wearable devices such as smartwatches and body-worn sensors. It has a detection range of up to 3x3 meters and can provide real-time data on the position and movement of the human body. The LD7903A module is equipped with several advanced features such as low phase noise and high sensitivity, which enable it to accurately detect and track human bodies even in complex environments. It also has a wide field of view and can detect movement in multiple directions simultaneously. The module communicates with the host system through a PWM input and can provide raw data or processed data, depending on the application. The LD7903A is designed for use in a variety of applications, including indoor navigation, security systems, and health monitoring.

3.3 Analyze the working principle and performance of the circuit board.

The board consists of several sensor modules, such as a ToF sensor, a millimeter wave radar detection module, a buzzer and two vibrators. The board also has a battery management chip and an Atmega328P chip that handles the signal processing and control

logic. The board can switch between two modes depending on the state of a switch: a low-power mode and an optional mode.

Figure 10 Demo Board B compare with Apple Watch (41mm)

In the low-power mode, the switch is short-circuited and the board switches off all sensor modules to save energy. The only component that is working in this mode is the battery management chip ADP5091ACPZ, which is responsible for collecting energy from a solar panel and storing it in a lithium battery. The ADP5091ACPZ chip has an ultra-low quiescent current of 16 *nA* and can operate with input voltages as low as 80 mV. This ensures that the board can harvest energy efficiently even in low-light conditions and prolong the battery life.

In the optional mode, the switch is broken and the board activates the ToF sensor and the millimeter wave radar detection module. These two sensors are used to detect the distance and position of obstacles and human bodies around the blind user. The ToF sensor is a VL53L0X module that uses a laser to measure the time-of-flight of light reflected by an object. The ToF sensor can measure distances up to 2 meters with an accuracy of +/- 3 *mm* and has a fast measurement rate of up to 50 *Hz*. The ToF sensor communicates with the Atmega328P chip via I2C protocol and sends the distance data to it.

The Atmega328P chip then processes the distance data and converts it into an acoustic frequency that corresponds to the distance of the obstacle. The Atmega328P chip uses a

PWM output to send this frequency to the buzzer. The buzzer then emits an audible frequency that indicates the distance of the obstacle to the blind user.

The millimeter wave radar detection module is a highly advanced LD7903A module that employs cutting-edge 79 *GHz* radar technology to detect moving objects within a remarkable range of 9 *meters* and at an impressive angle of 270 *degrees*. Notably, the millimeter wave radar detection module is equipped with sophisticated features that enable it to differentiate between left and right movement based on the phase difference of the received signal. This means that the module can accurately track the direction and position of moving objects, which makes it highly useful for detecting and distinguishing pedestrians and users compare with millimeter-wave radar that can only detect human presence in [18] a dynamic environment. The seamless communication between the millimeter wave radar detection module and the Atmega328P chip is achieved through a PWM input. The Atmega328P chip then receives and processes the position data sent by the millimeter wave radar detection module, which allows for the seamless integration of this advanced technology in the design of a watch. The LD7903A is another highly advanced 79*GHz* millimeter-wave high-frequency radar sensing module, which can accurately sense human presence, and even track the movement trajectory of users within a 3x3 meter range.

The Atmega328P chip then processes the position data and converts it into a vibration intensity that corresponds to the direction of the human body. The Atmega328P chip uses another PWM output to send this intensity to one of the vibrators, which are small DC motors that can vibrate at different speeds. The vibrators are attached to each side of a belt or a vest that is worn by the blind user. The vibrator then vibrates at an intensity that indicates the position of the human body to the blind user.

3.4 Advantages and disadvantages

During testing, I found a few flaws not only in the circuit board, but also in the 3D printed housing.

- The hinges in the mechanical design were too stiff and the solar cover and PCB were difficult to open and close. This affected the functionality and durability of the watch.

Figure 11 Hinges disconnected.

- The circuit design used a flick switch that could not be pressed down, which prevented the watch from easily switching between low-power mode and working mode.

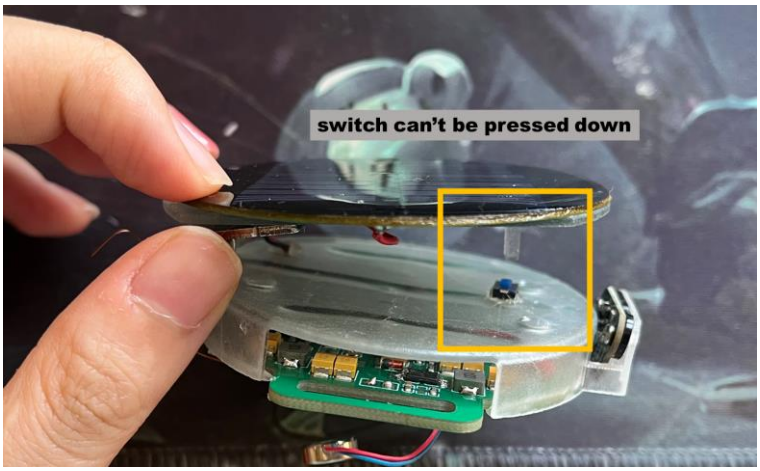

Figure 12 Improper switch selection

- The PCB design does not leave a row of pins for the ToF module to be soldered, which makes it very unstable and prone to flying wire disconnections. This compromised the accuracy and reliability of the distance measurement function.

- The two vibration motors were not designed to be symmetrical to each other and the pins were too close together to alert the user of the direction. As a result, one of the motors had to be connected with flying wires, which could easily break during use. This reduced the effectiveness and consistency of the tactile feedback function.

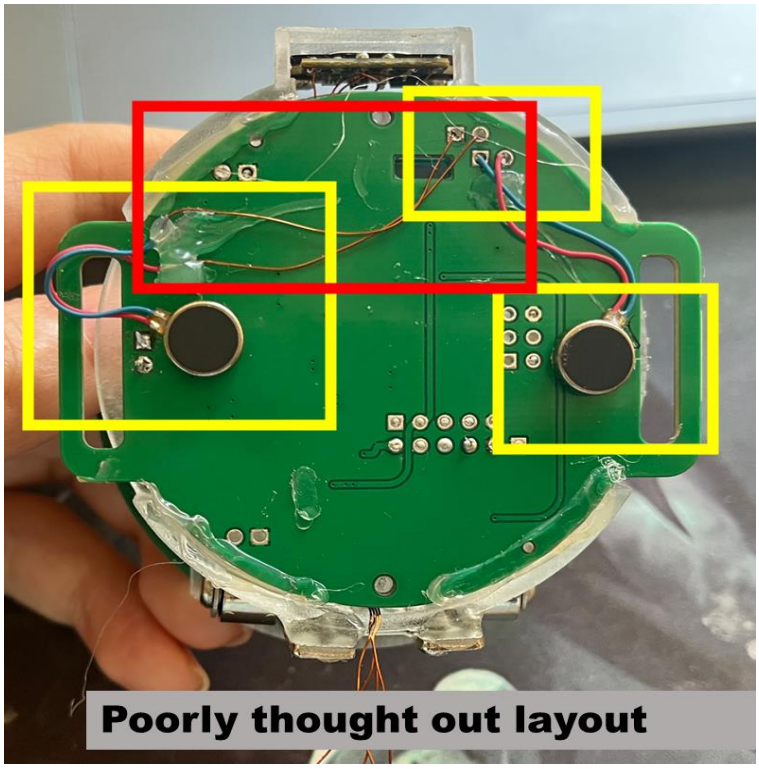

Figure 13 Component Place error

4 Watch Version C

4.1 Describes the function and purpose of the board.

To open and close the solar cover and PCB, gently press on the hinges to release the latch. A flexible hinge has been added to improve functionality and durability. And to switch between low-power mode and working mode, I use the Hall switch. In the previous version, a flick switch was used, which could not be easily pressed down. However, in this version, a Hall switch with low power consumption has been added, which can detect the light intensity and switch modes accordingly. When soldering the Time-of-Flight (ToF) module, I use the extra row of pins. In the previous version, the PCB design did not leave a row of pins for the ToF module, which made it unstable and prone to Flying wire disconnections. However, in this version, an extra row of pins has been added to the ToF module to ensure stability and accuracy. When connecting the vibration motors, they are symmetrical and have enough space for their pins. In the previous version, the two vibration motors were not designed to be symmetrical, and the pins were too close together. This made it difficult to alert the user of the direction, and one of the motors had to be connected with flying wires. However, in this version, the PCB layout has been redesigned

to ensure that the two motors are symmetrical and have enough space for their pins. Table 6 shows the BOM of the Watch Version C circuit diagram, and Figure 22 Figure 23 and Figure 24 show the schematic diagram of the Watch Version C.

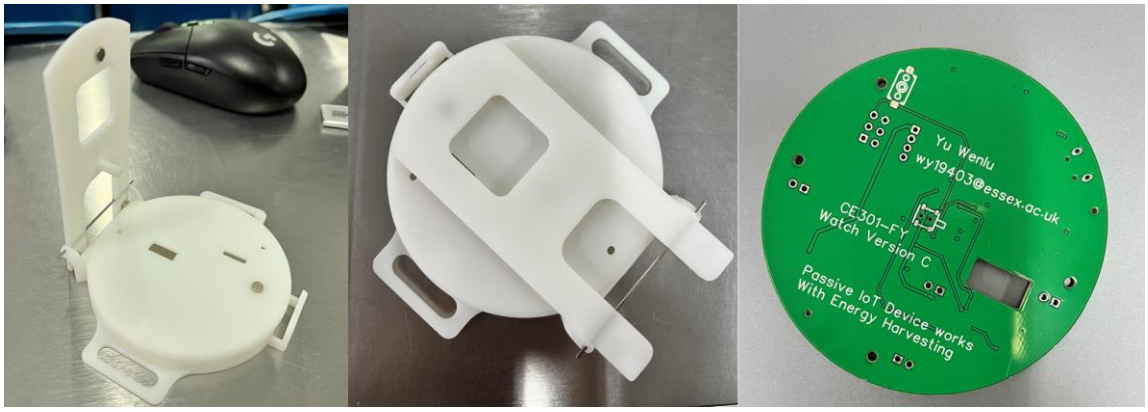

Figure 14 Watch Version C 3D print Case model and PCB

4.2 Explain the main components and devices on the circuit board.

Compare with Demo Board B, I incorporated **three switches** to enhance the functionality of the watch. The first switch is located on the front of the PCB board, and two switches are on the back of the PCB board, as shown in the right figure of Figure 15. The Hall switch is positioned on the front of the PCB, and there is a magnet behind the solar cover. When the magnet on the solar backboard is close to the Hall switch on the front of the PCB, the Hall switch will send a high-level signal to the Atmega328P microcontroller.

The main control chip will then turn off all sensors and enter low power consumption mode. This feature is highly beneficial for conserving battery life, as it allows the watch to enter power-saving mode when it is not being worn or is in a dark environment. Additionally, the Hall switch is highly reliable and accurate, ensuring that the watch enters low power mode only, when necessary, thereby prolonging its battery life. To provide users with a smooth and effortless experience, I added a reset switch during debugging. I chose the K2-3.6×6.1_SMD keyboard switch as it is not only easy to use but also allows for quick debugging through the console. In addition, I added another switch to detect whether the user is wearing the watch on their hand. For this switch, I selected the ESE13V01A light touch switch. This switch has a high level of reliability and durability, ensuring the longevity of the device. The pressure sensor on this switch helps to accurately determine whether the user is wearing the watch on their wrist, and can quickly reset the device if the watch is taken off. With all these switches, my watch

design can provide users with an exceptional experience.

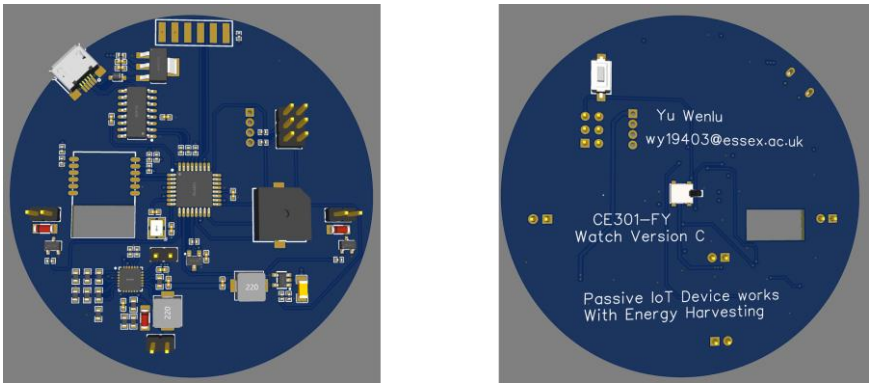

Figure 15 Watch Version C PCB 3D rendering Model

In addition, I added **a USB-burned PCB circuit board** to enable easy programming and communication with the Atmega328P microcontroller, improving the convenience and efficiency of programming [20]. Compared to the Demo Board B, this feature provides a significant advantage. The USB programming module is comprised of several key components, including a Micro-B USB interface that supports the USB 2.0 standard. This connector enables the circuit board to connect to a computer and provides 5V power and high-speed data transmission for programming and communication. The USB programming module includes an SPI interface, which is a serial peripheral interface that is necessary for programming the Atmega328P. This interface needs to be connected to the MISO, MOSI, SCK, and RESET pins to enable efficient programming. Additionally, a crystal oscillator circuit is used to generate a stable clock frequency for the Atmega328P. To ensure optimal performance, a 16*MHz* crystal and two 22*pF* load capacitors are required. The power supply filter is another essential component of the USB programming module. It is responsible for filtering out high-frequency noise and clutter in the power input, ensuring the normal operation of the circuit board. A 10uF electrolytic capacitor and a 0.1uF ceramic capacitor are required to enable effective power supply filtering. Meanwhile, to prevent electrostatic discharge and power noise interference, several protection components are included in the USB programming module. These components include a 10k ohm pull-up resistor, a 100 *ohm* current limiting resistor, and a diode. These components work together to ensure that the circuit board is protected from potential damage caused by electrostatic discharge and power noise interference.

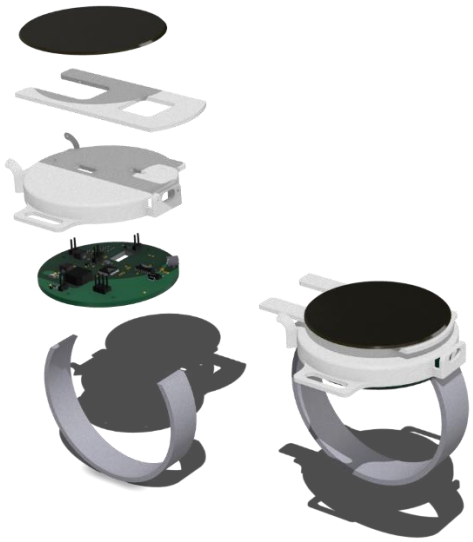

Figure 16 Watch Version C Physical rendering 3D model.

4.3 Analyze the working principle and performance of the circuit board.

The operation of the solar-powered watch circuit board can be summarized in the following steps:

- When the light touch switch is closed, indicating that the user is wearing the watch, the main control chip is powered on and starts to work.
- If the solar cover is closed, the Hall switch sends a high-level signal to the main control chip, which turns off all sensors except the battery management chip. The battery management chip continues to work and stores the collected solar energy as electrical energy, while also outputting a stable voltage to the main control chip.
- If the solar cover is opened, the main control chip activates all sensors, including the millimeter-wave radar and ToF sensor, and enters the working mode. The battery management chip continues to output a stable voltage and harvest solar energy.
- The millimeter-wave radar detects the surrounding environment, including the presence of human bodies, and sends the data back to the main control chip. The main control chip distinguishes between users and pedestrians (vehicles) based on the trajectories of multiple human bodies detected by the millimeter-wave radar. When detecting pedestrians (vehicles) approaching, the main control chip judges the distance and speed of other people relative to the user according to the trajectory data and outputs PWM waves to drive the front/rear motor to remind the user of the

corresponding direction of the pedestrian.

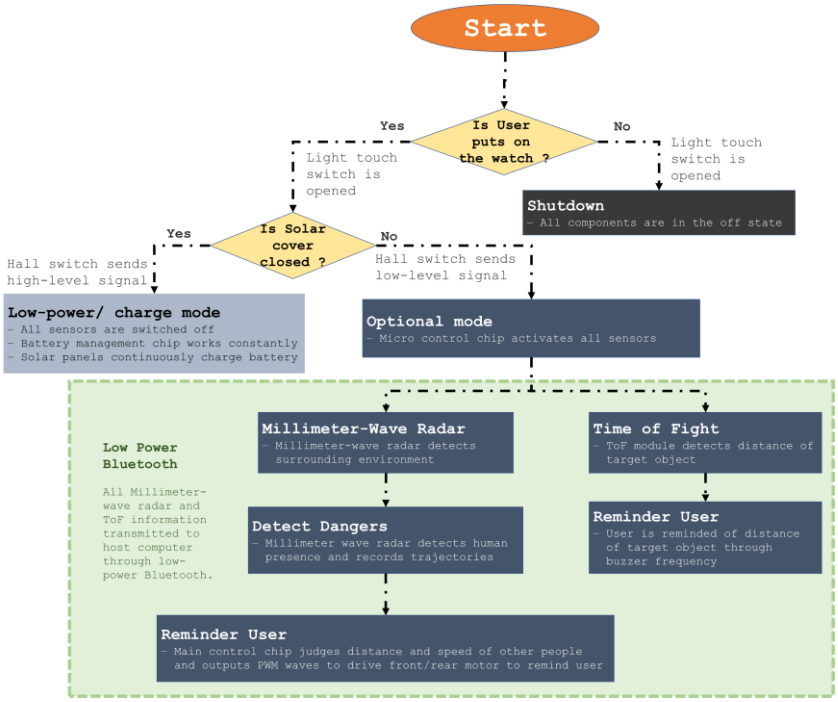

Figure 17 Watch Version C Workflow Chart

- The ToF module detects the distance of the target object and reminds the user of the distance of the target object through the frequency of the buzzer.
- All debugging information can be transmitted to the host computer through the low-power Bluetooth module to facilitate debugging.
- If the user removes the watch, the light touch switch is opened, and the main control chip enters the low-power standby mode until the user wears the watch again.

Chapter4. Results

1 Detection Results

To test the detection effect of millimeter-wave radar, we conducted experiments in different scenarios. The millimeter wave radar will send the coordinates (X, Y) and time stamp of the detected human body movement back to the main control chip through the SPI protocol (the coordinates of the wearer are always 0, 0), and we can pass the Bluetooth low energy module to the data acquired in real time is transmitted to the host computer. Table 7 Millimeter wave Radar data Preview shows a set of typical data samples. To analyze the returned data more intuitively, we used a scatter plot to statistically draw it, and Figure 18 Multi-person trajectory drawing scatter plot shows a visual display of the sensor data. Figure 18 1-4 show the movement trajectories of two distinct targets when the wearer is at rest (the yellow dash represents pedestrian 1 and the red dash represents pedestrian 2). In this case, the sensor output contains only a small amount of noise signal generated by other obstacles and the circuit itself, and it can be clearly observed that target 2 is moving to the right. Figure 18 5-8 shows the signal output by the sensor when the wearer is in motion. In this case, it can be seen from the graph that there are many scattered signals that are not connected into a line containing a lot of noise and the trajectory of the object being detected fluctuates a lot.

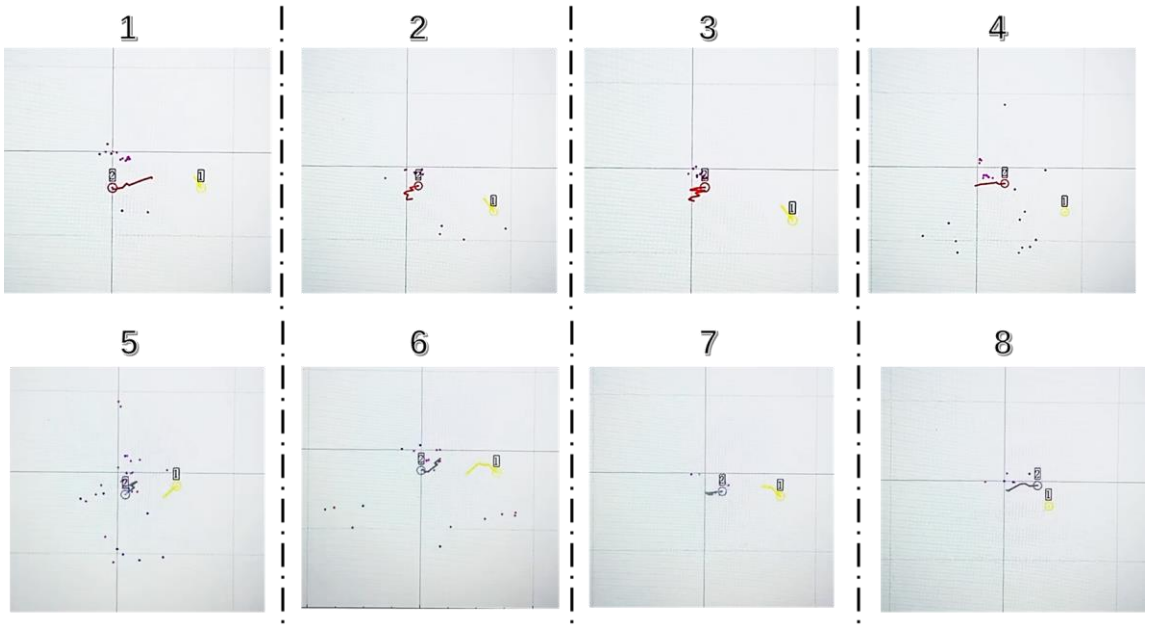

Figure 18 Multi-person trajectory drawing scatter plot

2 Energy Harvest

The testing and selection of energy sources were carried out for the development of a wearable device. Two energy sources, thermoelectric generator and solar panels, were evaluated and tested to determine their suitability for the device.

Thermoelectric generator:

The thermoelectric generator (TEG) products are made of ceramic material, which enables fast heat transfer. However, it is challenging to design a heat dissipation structure to maintain temperature difference in small wearable products, and the energy generated is extremely small. The test results from the handbook of the most commonly used TEG material Bi2Te3 showed (Figure 19) that only about 0.3V voltage can be generated under a temperature difference of 20 degrees Celsius, and the conversion efficiency is less than 2%. Regardless of being a hot end or a cold end, the temperature difference between the human body surface and the environment cannot reach 20 degrees Celsius in most cases. Hence, it can only generate weak power when the user wears it and cannot continue to power the device after being put down by the user. Therefore, thermoelectric sheets are not suitable for practical applications in wearable devices.

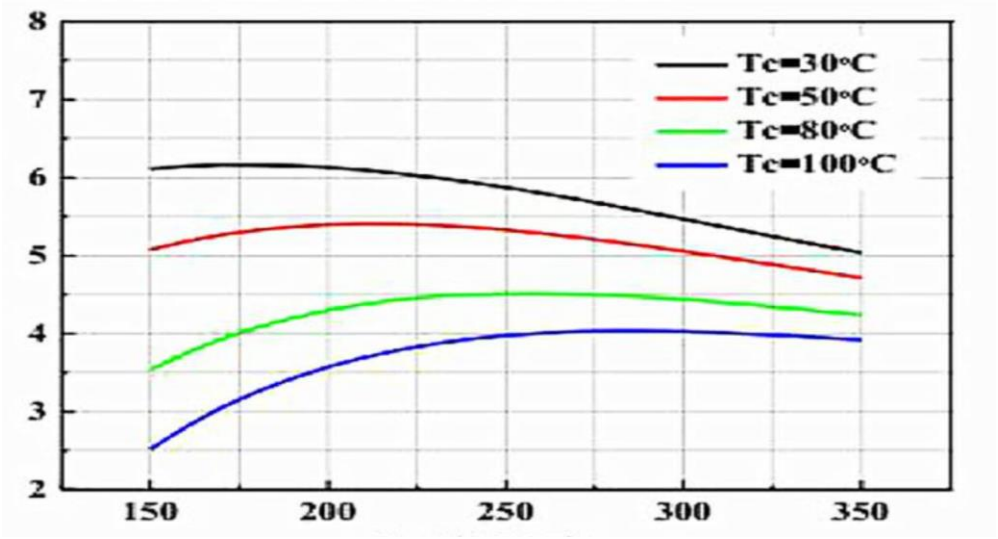

Figure 19 Effect of different hot junction temperature on TEG collection voltage

Solar panels:

Solar panels have certain requirements for the use environment, but in most outdoor situations, the power supply of solar panels is sufficient to maintain the operation of the

equipment and store the excess power in the battery. Two types of solar panels, flexible amorphous silicon and rigid polycrystalline/multi-crystalline silicon were tested to determine their suitability for the device.

After testing, it was found that the flexible solar panel made of amorphous silicon can generate electricity under extremely weak light but cannot produce high-power output even under strong light. The rigid solar panels are divided into polycrystalline silicon and monocrystalline silicon. Polycrystalline silicon has better weak light performance than monocrystalline silicon, but monocrystalline silicon has the highest output power under strong light. To continuously supply power to the equipment, the open circuit voltage, maximum power point voltage, and maximum output power of polycrystalline silicon and amorphous silicon solar panels were compared and tested under similar lighting conditions. The test results showed that polysilicon materials can produce several times higher power per unit area than amorphous silicon materials under strong outdoor light. Since it is inconvenient to wear large-area flexible solar panels, polysilicon rigid solar panels were finally selected as the energy source for the wearable device.

3 Overall

After rigorous testing and improvements based on the feedback from Methodology, the Watch Version C emerged as the final product of this project, with enhanced functionalities and performance. The final design of the watch is showcased in Figure 20, highlighting the sleek and lightweight form factor that was prioritized to ensure user comfort and aesthetics.

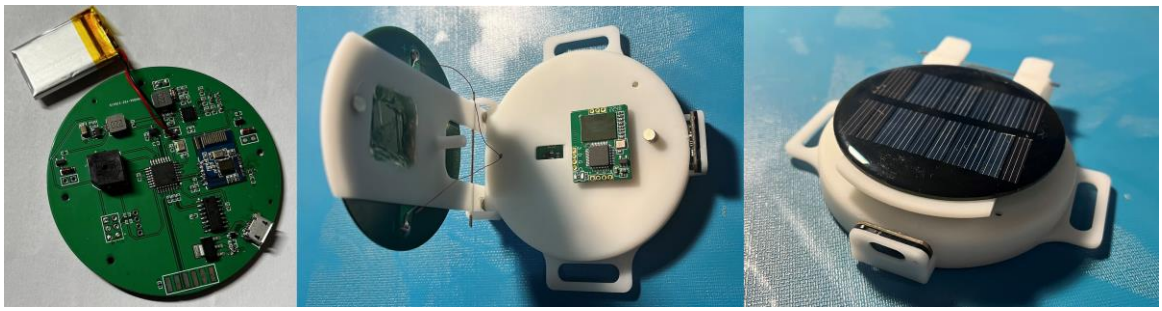

Figure 20 Watch Version C Physical photograph

To assess the effectiveness of the watch, several realistic simulations were carried out where the user was blindfolded and asked to drive indoors, outdoors, on a narrow road with two obstacles, two pedestrians, and a car passing by. The watch was activated by

opening the lid and entering an optional mode, which triggered the millimeter wave sensor, low-power Bluetooth module and ToF to start working seamlessly. To provide readers with a clear understanding of the testing methodology, Table 1 shows the coordinates of the obstacles at different timestamps in each scene. The coordinates of the wearer were always set to (0, 0), and the user was instructed to move slowly at a constant speed from east to west in all four scenarios. This allowed us to accurately measure the performance of the watch's features in each situation. It is important to note that the data presented in each scene is for demonstration purposes and is not representative of the full dataset. Only a portion of the actual data has been intercepted and is included in this study.

Table 1 Real-time coordinates of pedestrians, cars and obstacles in different scenes

Scenario	Time stamp	Actual distance (X, Y)				
		Obs 1	Obs 2	Ped 1	Ped 2	Car
1. Indoor, two stationary obstacles	0:00:37	2, 8.4	53.6, -0.3			
	0:01:09	2.2, 8.2	48.9, -0.6			
	0:01:28	1.7, 8.1	43.5, -0.5			
	0:01:57	1.2, 8.4	41.8, -0.6			
2. Outdoor, two pedestrians	0:00:42			12.3, -71.9	80.4, 23.7	
	0:01:15			11.8, -64.3	81.9, 19.1	
	0:02:02			9.9, -60.1	81.8, 15.4	
	0:02:44			9.3, -58.8	81.9, 10.1	
3. Outdoor, two pedestrians, two stationary obstacles	0:00:28	-71.2, -13.1	43.1, -55.8	29.7, -54.3	-91.8, 0.2	
	0:00:58	-73.4, -13.5	42.2, -52.4	30.2, -47.2	-83.5, 0.4	
	0:01:49	-76.8, -13.2	42.4, -50.1	31.5, -34.8	-76.0, 0.0	
	0:03:13	-79.1, -12.9	43.6, -47.6	32.0, -27.9	-65.3, 0.1	
4. Outdoor, two pedestrians, one car, two stationary obstacles	0:00:10	-37.8, 47.8	7.3, 1.2	21.9, -40.1	-14.8, 0.8	9.1, 154.9
	0:00:54	-37.5, 45.6	6.5, 0.8	18.8, -38.5	-9.1, 0.2	8.7, 112.3
	0:01:25	-37.6, 43.9	4.8, 0.4	15.3, -25.4	-3.2, 0.0	8.3, 84.8
	0:01:50	-37.4, 41.0	3.1, 0.2	13.6, -20.1	-0.2, 0.1	9.1, 43.7
	0:02:14	-37.3, 39.9	2.4, 0.1	10.2, -9.3	1.0, -0.1	9.8, 0.2
	0:02:57	-37.7, 38.1	0.9, -0.1	7.1, -2.4	2.5, -0.2	10.8, -20.9
	0:03:20	-37.8, 35.8	0.1, -0.3	2.3, 3.7	6.1, -0.1	11.7, -47.1

The form is divided into four scenarios, each of which is described in detail. The first scenario involves driving indoors while blindfolded and navigating through two stationary

obstacles. The second scenario involves navigating through two pedestrians in an outdoor environment. The third scenario tests the watch's ability to detect and alert users about two pedestrians and two stationary obstacles in an outdoor environment. The fourth scenario includes two pedestrians, one car, and two stationary obstacles in an outdoor environment.

The ToF module measures the distance and returns this value $\boldsymbol{D_{ToF}}$ between the wearer and an obstacle. Meanwhiles, we have used the Pythagorean theorem (Equation 1) based on the $\boldsymbol{X_{ToF}}$, $\boldsymbol{Y_{ToF}}$ coordinates of the obstacle measured by the laser rangefinder.

$$D_{act} = \sqrt{{X_{ToF}}^2 + {Y_{ToF}}^2}$$

Equation 1 Pythagorean theorem

We then compared this value to the distance obtained by the ToF module and calculated the accuracy using Equation 2. This allowed us to determine the ToF module's accuracy in detecting obstacles and measuring distances.

$$Accuracy_{\ ToF} = 1 - \frac{|D_{ToF} - D_{act}|}{D_{act}}$$

Equation 2 ToF Accuracy calculate formula

The same applies when testing millimeter wave radars, The millimeter wave radar module, on the other hand, measures the real-time coordinates of pedestrians in $\boldsymbol{X_{Mil}}$ and $\boldsymbol{Y_{Mil}}$. To calculate the accuracy of the millimeter wave radar module, we compared the actual coordinates of the pedestrian($\boldsymbol{X_{Mact}}$ and $\boldsymbol{Y_{Mact}}$.) to the return values from the module. We then calculated the accuracy of the *X* and *Y* coordinates separately (Equation 3) and took the average value as the result.

$$Accuracy_{\ Y-Mil} = 1 - \frac{|Y_{Mil} - Y_{Mact}|}{Y_{Mact}}$$

Equation 3 Millimeter wave radar Y axis Accuracy calculate formula

Table 2 illustrate the accuracy of the data received by each sensor module compared to the actual data at different timestamps. The scenarios were designed to test the watch's ability to detect and alert users about various obstacles such as stationary objects, pedestrians, and cars. To distinguish the accuracy of the sensor in various scenarios, I have employed a color-coded approach for each table. The background colour of each table corresponds to the accuracy of the current accuracy value when compared against

the same type of obstacle, including pedestrians, vehicles, and static obstacles. A gradient ranging from green to red is used to indicate the level of accuracy, with green representing higher accuracy and red indicating lower accuracy. By using this visual aid, readers can quickly and easily discern the performance of the sensor in each obstacle.

Table 2 Accuracy of pedestrians, cars and obstacles for different sensors

Scenario	Time stamp	ToF Accuracy (%)		Millimeter Accuracy (%)		
		Obs 1	Obs 2	Ped 1	Ped 2	Car
1. Indoor, two stationary obstacles	0:00:37	91.8045238	95.251362			
	0:01:09	97.7025667	94.838037			
	0:01:28	98.5312136	94.76009			
	0:01:57	98.9234193	93.202298			
2. Outdoor, two pedestrians	0:00:42			97.239151	95.262452	
	0:01:15			95.473768	87.52235	
	0:02:02			93.518733	99.945384	
	0:02:44			93.834121	87.992592	
3. Outdoor, two pedestrians, two obstacles	0:00:28	95.5583635	97.32288	92.541594	84.760121	
	0:00:58	96.9720263	92.102694	89.355507	91.739309	
	0:01:49	93.2425181	97.906064	85.915765	87.787359	
	0:03:13	92.9346153	97.772864	90.488576	92.075507	
4. Outdoor, two pedestrians, one car, two obstacles	0:00:10	93.8535791	95.60971	82.705807	86.843978	76.7457041
	0:00:54	98.5909629	94.35173	81.034531	84.786191	78.6584446
	0:01:25	92.0968918	96.743778	92.859767	89.279527	77.6150074
	0:01:50	91.4991226	95.215465	83.353578	80.900986	77.5057855
	0:02:14	97.0675494	99.481882	84.865659	92.718884	76.5452513
	0:02:57	98.2890162	98.369559	90.38312	89.666464	83.5483136
	0:03:20	98.4711368	98.923419	90.130163	91.625164	85.7272909

Based on the analysis presented in the table above, it can be inferred that the Time of Flight (ToF) technology displays higher accuracy than the millimeter-wave radar, with minimal influence from the environment. The ToF technology exhibits a minimum accuracy of 91% and a maximum accuracy of 99%, which is significantly higher than the millimeter-wave radar. However, the precision of ToF measurements is largely dependent on the distance between the sensor and the object under consideration. The experimental results from scenarios 1, 2, and 3 indicate that the ToF sensor is more accurate at measuring the objects located at closer distances as opposed to the objects

that are further away.

Compared to the ToF sensor, the millimeter wave radar sensor exhibits lower accuracy in detecting multiple human presence tracking and converting it to coordinates in real time. Moreover, its accuracy is further reduced in different scenarios as the number of obstacles increases. The second scenario, with only two pedestrians around the wearer, showcases the millimeter wave radar sensor's commendable performance. The measured accuracy peaks at 99.95% at 0:02:02, with only two values falling below 90%, but still greater than 85%. However, in the more complex scenarios 3, with the addition of two static obstacles, the accuracy significantly drops compared to scenarios 2, despite having only two pedestrians around the wearer. Pedestrian 2 has the lowest millimeter wave radar accuracy of 83% at 0:00:28 in scenario 3, with all pedestrian 1 distances being below 90%.

Scenario 4 is by far the most intricate scenario with the presence of two pedestrians, a car, and two static obstacles. Unfortunately, the millimeter-wave radar struggles to accurately measure the pedestrians in this scenario compared to the previous ones. At 0:01:50, the lowest accuracy is recorded, with a measly 80% accuracy for pedestrian 2, significantly lower than what was achieved in Scenario 2 and 3. The measurement accuracy for the car (i.e., the driver) fares no better, with the lowest accuracy being a mere 76%, and even with the distance decrease between the vehicle and the user factored in, the measurement accuracy barely breaches 86%.

Project Planning

The whole project ran from October 2022 to mid-April 23. During this process, I mainly worked on module testing and Shield Board A modules during the first semester from October to December. During the first semester's progress, when I need to start an Epic, I will fill in the relevant information in Jira, add the sub-module and complete it as planned. In the second semester of the project process, I went ahead and added all the Epics to Jira and estimated a suitable time based on previous experience. Obviously, I finished the second semester higher than the first, but because I did not expect Demo Board B to meet all my needs in the second semester, I urgently designed and produced Watch Version C, which eventually completed all my needs.

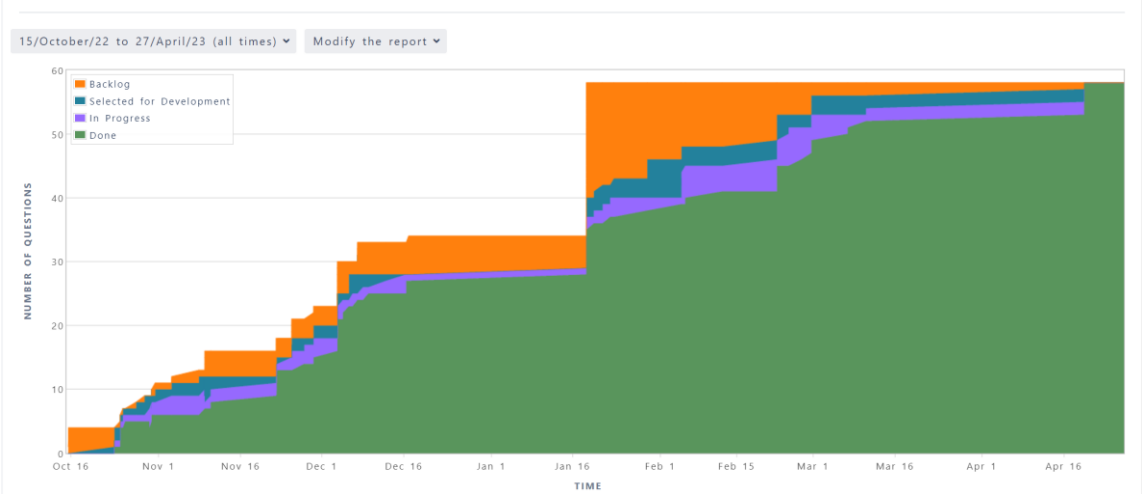

Figure 21 Jira Report for Whole Project

Regarding risk management, I used a risk matrix approach to assess the likelihood and impact of each risk and to determine the appropriate risk response strategy. I used Jira as risk management tools and techniques, regularly updated and reviewed my risk management plan, and communicated and coordinated with supervisors. I determine risk tolerance and risk appetite based on the project's objectives and expected outcomes, and try to balance risk and opportunity. I use metrics such as risk exposure and risk-return ratio to measure my risk management performance.

There were three risks that I did not anticipate that led to some negative consequences. Firstly, throughout the first semester of the project, due to various policy restrictions in

China for Covid-19, there were various delays and out-of-stock purchases of various components and PCBs online. This had an impact on the early module testing. To counter this risk, I promptly adjusted my purchasing plan and searched for alternative reliable suppliers. Secondly, during the first semester, I focused a lot of energy on the flexible thermoelectric and flexible solar panels, resulting in a lot of wasted time. Fortunately, Professor Hossein corrected this in time and advised me to use a simpler and more practical solution. To avoid this risk, I should have done more market research and technical analysis before starting to ensure that my solution met the project's requirements and budget. In the end, I did not review the "Demo Board B" version of the board carefully enough to think it through, resulting in an emergency design and production of "Watch Version C", which slowed down the overall schedule. To mitigate this risk, I accelerated my design and sought help and feedback from other students and my tutor.

There were three risks that I foresaw and managed well that brought some positive results. 1. When purchasing PCBs, components and 3D printed models, I always deliberately bought 50% more to ensure that progress would not be affected by unexpected damage to parts. 2. Delays. It turns out that when probing QFN packaged chips, the pins are too small and improper handling can burn out the chips and MOS tubes. 2. I made plan B for the main chip choice, using the Atmega328P instead of the NXP FRDM-K32L2B. so when designing the shield board in the beginning, I used the Arduino Rev3 pinout allowed the shield to fit the K32L2B development board and the Arduino Uno perfectly, so that when faced with the dilemma of developing the K32L2B, I could immediately turn to the Atmega328P chip and complete the requirements.

Conclusion

In this article, I have presented the design and implementation of Watch Version C, a smartwatch that can assist blind people in navigating urban environments safely and conveniently by using solar energy and millimeter wave radar technology. Through a systematic methodology that included module testing, shield board design, demo board design, and prototype evaluation, I have demonstrated the detection accuracy and energy harvesting efficiency of the watch prototype. By considering the user's comfort and aesthetics, I have created a lightweight and stylish watch that can combine multiple functions to improve the lives of blind people.

This project represents a significant step towards providing a reliable and convenient device that can help blind people avoid collisions with obstacles. It also highlights the potential of millimeter wave radar technology and energy harvesting technologies for wearable devices. The successful implementation of Watch Version C opens up new possibilities for further research and development in the field of smart wearable devices for blind people. Future work could focus on improving the detection range and resolution of the radar module, optimizing the energy management and provision system, and enhancing the user interface and feedback mechanism of the watch. This project has shown that with innovative thinking and careful design, wearable devices can be used to provide solutions to significant challenges faced by the visually impaired. It is my hope that the success of this project will inspire further research and development in the field and contribute to the creation of more smart wearable devices that can improve the lives of people with disabilities.

Reference

1 “Seebeck effect | physics | Britannica.,” [Online]. Available: https://www.britannica.com/science/Seebeck-effect. [Accessed 3 4 2023].

2 “I. P-Type, N-Type Semiconductors - Engineering LibreTexts.,” [Online]. Available: https://eng.libretexts.org/Bookshelves/Materials_Science/Supplemental_Modules_(Materials_Science)/Solar_Basics/D._P-N_Junction_Diodes/I._P-Type%2C_N-Type_Semiconductors.

3 Wikipedia, “Polydimethylsiloxane,” [Online]. Available: https://en.wikipedia.org/wiki/Polydimethylsiloxane. [Accessed 6 4 2023].

4 “UNO R3 | Arduino Documentation | Arduino Documentation.,” [Online]. Available: https://docs.arduino.cc/hardware/uno-rev3. [Accessed 17 4 2023].

5 “FRDM-K32L2B3 Platform|Freedom Development Board,” NXP Semconductor, [Online]. Available: https://www.nxp.com.cn/design/development-boards/freedom-development-boards/mcu-boards/nxp-freedom-development-platform-for-k32-l2b-mcus:FRDM-K32L2B3. [Accessed 15 4 2023].

6 “What is Maximum Power Point Tracking (MPPT) | NAZ Solar Electric.,” [Online]. Available: https://www.solar-electric.com/learning-center/mppt-solar-charge-controllers.html/ . [Accessed 31 3 2023].

7 I. C. Maker., “How Do the Blind Safely Cross the Road?,” inclusivecitymaker, [Online]. Available: https://www.inclusivecitymaker.com/how-do-the-blind-safely-cross-the-road/. [Accessed 29 2 2023].

8 G. P. L. G. A. T. a. M. T. A. Leonardi, “Powering smart wearable systems with flexible solar energy harvesting,,” *International Symposium on Circuits and Systems (ISCAS),*

pp. 1-4, May 2018.

9 Texas Instruments, The fundamentals of millimeter wave radar sensors (Rev. A), TX, USA, Application Report: Dallas,, 2018.

10 Y. L. Y. W. a. Y. Y. C. Xu, “Portable and wearable self-powered systems based on emerging energy harvesting technology,” *Microsystems & Nanoengineering,* vol. 6, no. 1, pp. 1-22, 2020.

11 G. Alexiou, "Sunu Band – The Smart Wearable Helping Blind People Maintain Social Distance," Forbes, [Online]. Available: https://www.forbes.com/sites/gusalexiou/2020/08/30/sunu-band--the-smart-wearable-helping-blind-people-maintain-social-distance/?sh=79d085c673be. [Accessed 11 3 2023].

12 R. Metzarchive, “A Smart Watch to Help Blind People Navigate,” MIT Technology Review, [Online]. Available: https://www.technologyreview.com/2017/08/04/150141/a-smart-watch-to-help-blind-people-navigate/. [Accessed 11 3 2023].

13 P. L. Q. L. Z. Z. S. H. Yifan Wang, “Design guidelines for chalcogenide-based flexible thermoelectric materials,” *ROYAL SOCIETY OF CHEMISTRY,* 14 3 2021.

14 M. Ray, Composer, *New Flexible and Wearable Thermoelectric + Solar Energy Harvesting Technology.* [Sound Recording]. YouTube. 2021.

15 H. M. Y. J. L. G. S. L. H. C. Y. J. K. S. H. L. S. H. C. a. B. J. C. Choong Sun Kim, “Self-Powered Wearable Electrocardiography Using a Wearable Thermoelectric Power Generator,” *ACS Energy Letters,* vol. 2018, no. 3,3, pp. 501-507, 2018.

16 S. Q. P. C. L. a. S. X. Yang, “Recent Developments in Flexible Thermoelectric

Devices.," *Small Sci.,* 2021.

17 "Industrial low power bluetooth module-PUSR IOT.," [Online]. Available: https://www.pusr.com/products/Industrial-low-power-bluetooth-module-WH-BLE106.html. [Accessed 1 4 2023].

18 "New Product Preview | Super cost-effective 24G human presence sensing radar HLK-LD2410," [Online]. Available: https://www.hlktech.com/NewsInfo-233.html. [Accessed 27 3 2023].

19 "High efficiency solar battery charger with embedded MPPT.," [Online]. Available: https://www.st.com/en/power-management/spv1040.html.

20 Simon, "Arduino as ISP and Arduino Bootloaders," Arduino, [Online]. Available: https://docs.arduino.cc/built-in-examples/arduino-isp/ArduinoISP. [Accessed 7 4 2023].

Appendices

Table 3 The performance of different types of solar panels.

Solar Panel	Open circuit voltage (V)	Maximum power point voltage (V)	Maximum power point current (mA)	Maximum output power (mW)
1 pcs Flexible Screen （266mm *140mm）*1	1.52	0.77	39.99	31.46
2 pcs Flexible Screen （266mm *140mm）*2	3.13	2.08	31.94	66.36
3 pcs Flexible Screen （266mm *140mm）*3	4.61	2.89	33.31	96.35
4 pcs Flexible Screen （266mm *140mm）*4	6.39	3.40	40.21	136.74
5 pcs Flexible Screen （266mm *140mm）*5	7.71	4.41	42.28	186.58
Rectangular rigid Screen (40mm * 40mm)	3.24	2.38	20.83	49.57
Circular rigid screen (R=32.5mm)	3.67	2.58	37.83	97.60

Table 4 BOM Shield Board A

ID	Value	Reference number	Quantity	Manufacturer Part	Manufacturer
1	K32L2_SHIELD	B1	1	K32L2B	NXP
2	HNB09A05	BUZZER2	1	HNB09A05	HuaNeng
3	22u	C1,C10	2		
4	0.1u	C2,C9	2		
5	1n	C3,C8	2		
6	330uF	C4,C7	2	RVT1V331M1010	ROQANG
7	100uF	C5	1	RVT1A101M0505	ROQANG
8	10u	C6	1		
9	2.54-2A-LT	CN21	1	2.54-2A-LT	CAX
10	HDR-F-2.54_1x6	H1	1		
11	HDR-M-2.54_1x2	J1,J2,J7,J8	4		
12	HDR-M-2.54_2x2	J3,J4,J5	3		
13	Motor_ENA	J6	1		
14	K2-3.6×6.1_SMD	KEY1,KEY2	2	K2-1107ST-A4SW-06	
15	10uH	L1,L3	2	MPH201612S100MT	Sunlord
16	22uH	L2	1	YNR2016-220M	YJYCOIN
17	19-217/GHC-YR1S2/3T	LED1	1	19-217/GHC-YR1S2/3T	EVERLIGHT
18	Z3OC1T8219731	M1,M2	2	Z3OC1T8219731	KOTL
19	SolarPanel	P1	1		
20	1k	R1,R4,R5,R7,R8,R9,R12	7		
21	160k	R2,R11	2		
22	68k	R3,R10	2		
23	10k	R6	1		
24	SPV1040TTR	U1,U6	2	SPV1040TTR	ST
25	ME2188A50XG	U2	1	ME2188A50XG	MICRONE
26	WH-BLE106	U3	1	WH-BLE106	null
27	LD2410	U4,U5	2	DW127R-11-05-34	DEALON
28	L9110S_C513306	U7,U9	2	L9110S	Mixic

Table 5 BOM Demo Board B

ID	Value	Reference number	Quantity	Manufacturer Part	Manufacturer
1	BS-08-B2AA016	BT1	1	BS-08-B2AA016	MYOUNG
2	FST-9650B-5V	BUZZER1	1	FUET-9650B-5V	FUET
3	10nF	C1,C3	2	CL05B103KB5NNNC	SAMSUNG
4	1uF	C2	1	CL05A105KA5NQNC	SAMSUNG
5	10uF	C4	1	CL05A106MQ5NUNC	SAMSUNG
6	100uF	C5	1	CL31A107MQHNNNE	SAMSUNG
7	0.1u	C6	1		
8	SS14	D1	1	SS14	MDD
9	ZMM3V3	D2,D3,D5	3	ZMM3V3-M	ST
10	Tof	H1	1		
11	PV	J1	1		
12	BAT	J2	1		
13	Vibrators-L	J3	1		
14	HDR-M-2.54_2x3	J4	1		
15	Vibrators-R	J6	1		
16	HDR-M-2.54_1x4	J7	1		
17	22uH	L1,L2	2	YSPI0530-220M	YJYCOIN
18	19-217/GHC-YR1S2/3T	LED1	1	19-217/GHC-YR1S2/3T	EVERLIGHT
19	S8050_C2146	Q1,Q4	2	S8050 J3Y	CJ
20	5.1MΩ	R1,R4,R5,R20,R21	5	0603WAF5104T5E	UNI-ROYAL
21	2.2MΩ	R2	1	0603WAF2204T5E	UNI-ROYAL
22	10k	R3,R6,R10,R11	4		
23	3MΩ	R7,R8,R9,R13	4	0603WAF3004T5E	UNI-ROYAL
24	2.7k	R12	1		
25	100kΩ	R14	1	0603WAF1003T5E	UNI-ROYAL
26	200kΩ	R17,R18	2	0402WGF2003TCE	
27	10MΩ	R19,R22	2	0603WAF1005T5E	UNI-ROYAL
28	TS-1187A-B-A-B	SW1,SW3	2	TS-1187A-B-A-B	UNI-ROYAL
29	ADP5091ACPZ-1-R7	U1	1	ADP5091ACPZ-1-R7	XKB Connectivity
30	LGT8F328P	U2	1	LGT8F328P	ADI
31	ME2188C50M5G	U3	1	ME2188C50M5G	MICRONE
32	UHE4913G-AE3-R	U4	1	UHE4913G-AE3-R	UTC
33	WH-BLE106	U6	1	WH-BLE106	

Table 6 BOM Watch Version C

ID	Value	rence nu	Quantity	Manufacturer Part	Manufacturer
1	FST-9650B-5V	BUZZER1	1	FUET-9650B-5V	FUET
2	10nF	C1,C3	2	CL05B103KB5NNNC	SAMSUNG
3	1uF	C2,C12,C13	3	CL05A105KA5NQNC	SAMSUNG
4	10uF	C4	1	CL05A106MQ5NUNC	SAMSUNG
5	100uF	C5	1	CL31A107MQHNNNE	SAMSUNG
6	0.1u	C6,C9,C10,C11	4		
7	15pF	C7,C8	2	0402CG150J500NT	FH
8	1N5819WS	D1	1	1N5819WS	Hottech
9	ZMM3V3	D2,D3,D5	3	ZMM3V3-M	ST
10	Tof	H1	1		
11	PV	J1	1		
12	BAT	J2	1		
13	Vibrators-L	J3	1		
14	ICSP	J4	1		
15	Vibrators-R	J6	1		
16	HDR-M-2.54_1x4	J7	1		
17	ESE13V01A	KEY1	1	ESE13V01A	PANASONIC
18	K2-3.6×6.1_SMD	KEY2	1	K2-1107ST-A4SW-06	
19	22uH	L1,L2	2	YSPI0530-220M	YJYCOIN
20	S8050_C2146	Q1,Q4	2	S8050 J3Y	CJ
21	5.1MΩ	R1,R5,R20,R21	4	0603WAF5104T5E	UNI-ROYAL
22	2.2MΩ	R2	1	0603WAF2204T5E	UNI-ROYAL
23	0R	R3,R25,R26,R28,R30,R31,R32	7		
24	10k	R6,R11,R27	3		
25	3MΩ	R7,R9,R13	3	0603WAF3004T5E	UNI-ROYAL
26	100k	R10,R24,R29	3		
27	2.7k	R12	1		
28	100kΩ	R14	1	0603WAF1003T5E	UNI-ROYAL
29	1k	R15,R16,R23	3		
30	200kΩ	R17,R18	2	0402WGF2003TCE	UNI-ROYAL
31	10MΩ	R19,R22	2	0603WAF1005T5E	UNI-ROYAL
32	ADP5091ACPZ-1-R7	U1	1	ADP5091ACPZ-1-R7	ADI/LINEAR
33	ATMEGA328P-AU	U2	1	ATMEGA328P-AU	MICROCHIP
34	ME2188C50M5G	U3	1	ME2188C50M5G	MICRONE
35	UHE4913G-AE3-R	U4	1	UHE4913G-AE3-R	UTC
36	CH340C	U5	1	CH340C	WCH
37	PW05	U6	1		
38	AMS1117-3.3	U7	1	AMS1117-3.3	AMS
39	U254-051T-4BH83-S1S	USB1	1	U254-051T-4BH83-S1S	XKB Connectivity
40	16MHz	X1	1	X322516MLB4SI	YXC

Table 7 Millimeter wave Radar data Preview

Object 1			Object 2		
Object Coordinates X	Object Coordinates Y	Time stamp	Object Coordinates X	Object Coordinates Y	Time stamp
45.37181465	-13.78090518	0:00:01	25.88250291	-15.59092156	0:00:01
45.4059303	-13.82712611	0:00:03	25.69496554	-15.69897317	0:00:03
45.44058368	-13.84587442	0:00:05	25.30886199	-15.79442575	0:00:05
45.4830881	-13.878496	0:00:07	25.1218904	-15.89249247	0:00:07
45.58535049	-13.90641748	0:00:09	24.88825961	-15.99905422	0:00:09
45.64410253	-13.93256446	0:00:11	24.50624292	-16.09123875	0:00:11
45.72814629	-13.96323942	0:00:13	24.21098549	-16.19925685	0:00:13
45.76129687	-13.99427293	0:00:15	24.0368752	-16.29340179	0:00:15
45.78934741	-14.02846762	0:00:17	23.71886212	-16.39400382	0:00:17
45.82526107	-14.05423304	0:00:19	23.49714781	-16.49219136	0:00:19
45.88651453	-14.08591185	0:00:21	23.10006971	-16.59067822	0:00:21
45.95377847	-14.11345955	0:00:23	22.91439568	-16.69093647	0:00:23
46.06568118	-14.14051527	0:00:25	22.59314861	-16.79435706	0:00:25
46.1139699	-14.17963599	0:00:27	22.25422972	-16.89088616	0:00:27
46.12640437	-14.20155382	0:00:29	22.01710765	-16.99927827	0:00:29
46.21114802	-14.23122588	0:00:31	21.67167207	-17.09473858	0:00:31
46.33268788	-14.26258898	0:00:33	21.49943911	-17.19386063	0:00:33
46.31794959	-14.29385306	0:00:35	21.1890271	-17.29849452	0:00:35
46.38044175	-14.32512714	0:00:37	20.84475846	-17.39535049	0:00:37
46.43129878	-14.35716818	0:00:39	20.64748343	-17.49273599	0:00:39
46.54782128	-14.38946373	0:00:41	20.42910497	-17.59960239	0:00:41
46.58551139	-14.41326486	0:00:43	20.04222042	-17.69729498	0:00:43
46.64495495	-14.44128961	0:00:45	19.73848841	-17.79013708	0:00:45
46.6864556	-14.47216227	0:00:47	19.50610392	-17.89545902	0:00:47
46.72705506	-14.50524996	0:00:49	19.15733071	-17.99394732	0:00:49
46.8207891	-14.53945688	0:00:51	18.89243043	-18.09141954	0:00:51
46.86103061	-14.56580829	0:00:53	18.61091886	-18.1953281	0:00:53
46.91231695	-14.59262443	0:00:55	18.30106393	-18.29904688	0:00:55
47.00663937	-14.62092444	0:00:57	18.11255822	-18.39462229	0:00:57
47.09451611	-14.6533873	0:00:59	17.8600518	-18.49963219	0:00:59
47.11880632	-14.68788291	0:01:01	17.56992058	-18.59666279	0:01:01
47.1691021	-14.71229873	0:01:03	17.31744194	-18.69103174	0:01:03
47.20532364	-14.74829471	0:01:05	16.91475678	-18.7989911	0:01:05
47.26293854	-14.77059654	0:01:07	16.72765728	-18.89262573	0:01:07
47.41685958	-14.80127786	0:01:09	16.46559633	-18.99910309	0:01:09
47.47992526	-14.83092227	0:01:11	16.10249566	-19.09030502	0:01:11
47.50507371	-14.86618218	0:01:13	15.82200272	-19.19123695	0:01:13
47.53439158	-14.89979903	0:01:15	15.63675783	-19.2975959	0:01:15
47.65172643	-14.92568568	0:01:17	15.27654584	-19.39221077	0:01:17
47.70463392	-14.95393345	0:01:19	15.03245407	-19.49379558	0:01:19
47.72706495	-14.98266319	0:01:21	14.798518	-19.59230007	0:01:21
47.82152702	-15.01284878	0:01:23	14.4706443	-19.69954897	0:01:23
47.86464818	-15.0427169	0:01:25	14.19942335	-19.79545118	0:01:25
47.8657795	-15.07763743	0:01:27	13.86922142	-19.89448251	0:01:27
47.96584897	-15.10057051	0:01:29	13.67666058	-19.99255325	0:01:29
48.07352118	-15.13501851	0:01:31	13.35783978	-20.09728337	0:01:31
48.12861369	-15.1681498	0:01:33	13.05484354	-20.19297125	0:01:33
48.11114795	-15.1990057	0:01:35	12.79588326	-20.29624773	0:01:35
48.20811453	-15.22520808	0:01:37	12.53907455	-20.39561632	0:01:37
48.23149964	-15.25885722	0:01:39	12.21418566	-20.49881161	0:01:39

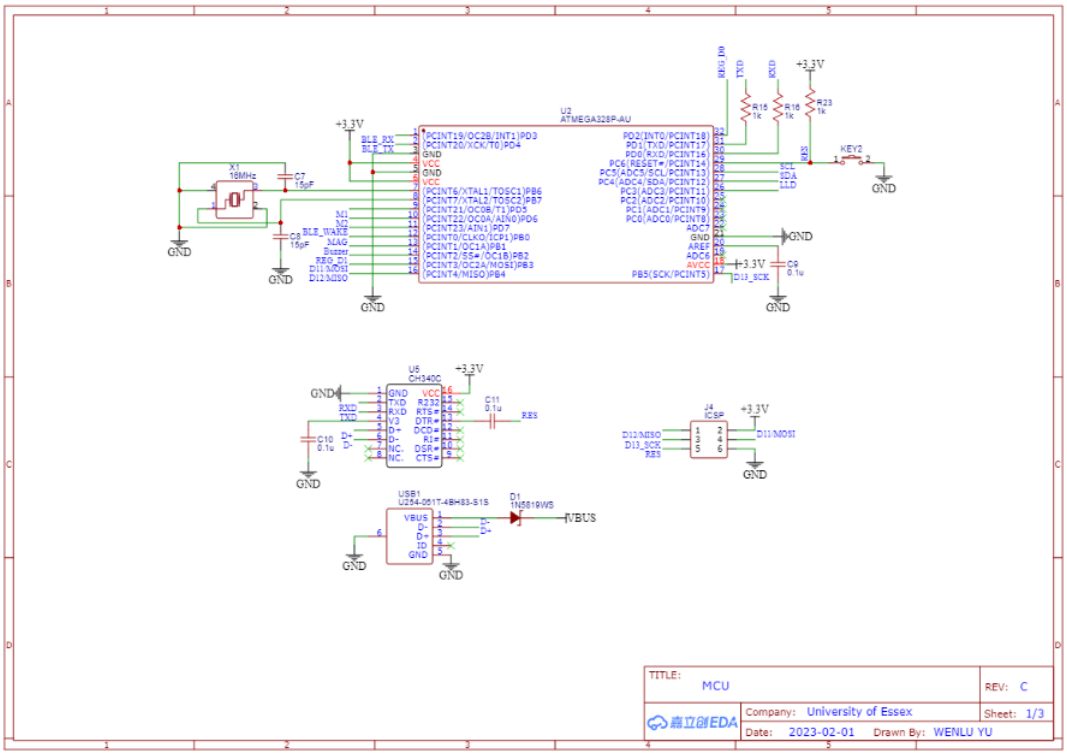

Figure 22 Schematic Watch Version C – MCU

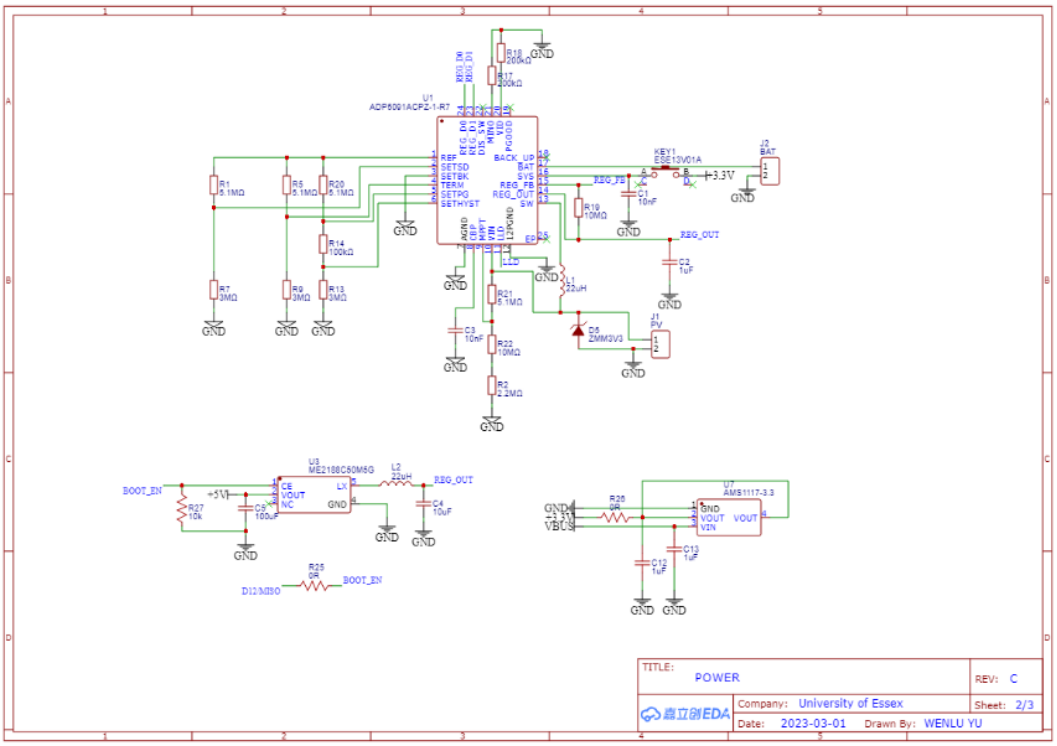

Figure 23 Schematic Watch Version C - Power

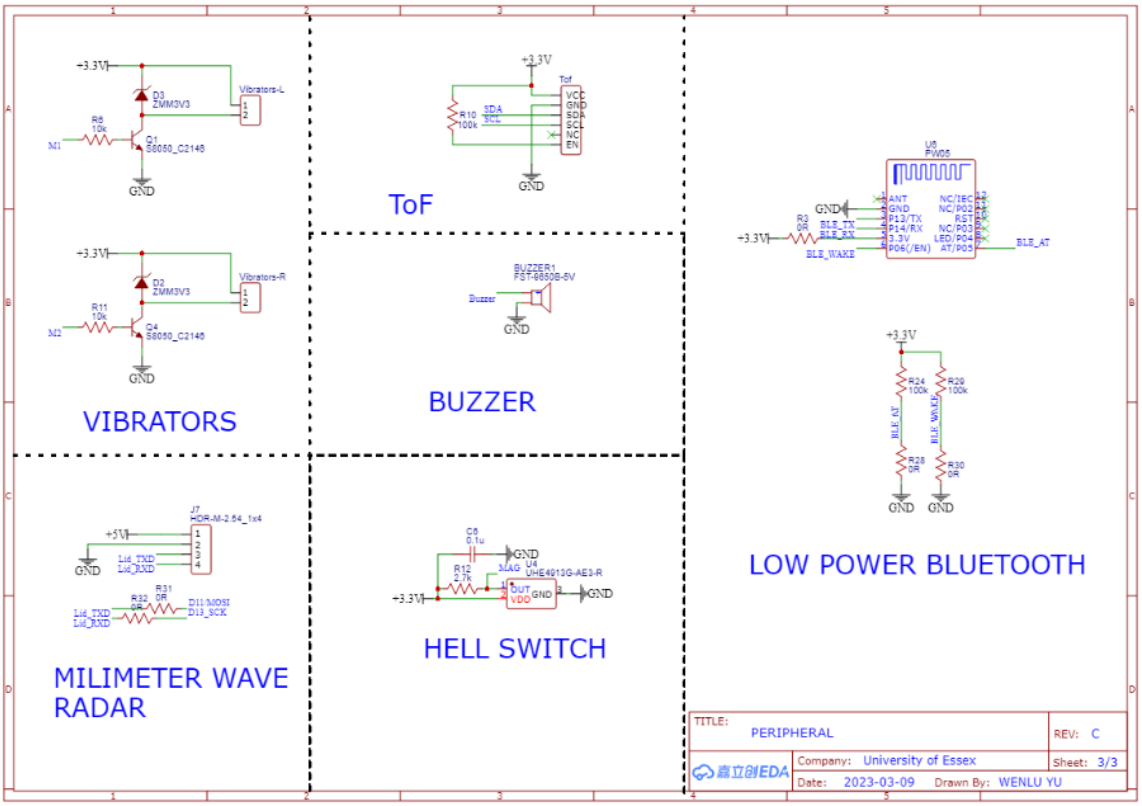

Figure 24 Schematic Watch Version C – Peripheral

Code

```
1.  // Yu Wenlu, 2023-03-21
2.  // wy19403@essex.ac.uk
3.  // This is a test code for the Watch_RTOS project.
4.  // The code is based on the example code of the Adafruit VL53L0X an
d Arduino_FreeRTOS library.
5.  // Using the VL53L0X to detect the distance between the watch and t
he user's hand.
6.  // Using the Arduino_FreeRTOS library to create two tasks, one for
the distance detection and the other for the buzzer.
7.
8.  #include <Arduino_FreeRTOS.h>
9.  #include "Adafruit_VL53L0X.h"
10.
11.  // define two tasks for Blink & AnalogRead
12.  void TaskBlink( void *pvParameters );
13.  void TaskAnalogRead( void *pvParameters );
14.
15.  //define variables
16.
17.  int Beep_Duration = 100;
18.  int Buzzer_pin = 9;
19.  bool close_to = false;
20.  int pos_x = 0;
21.  int pos_y = 0;
22.  VL53L0X_RangingMeasurementData_t measure;
23.  Adafruit_VL53L0X lox = Adafruit_VL53L0X();
24.
25.  // the setup function runs once when you press reset or power the b
oard
26.
27.  void setup() {
28.    pinMode(8,INPUT);
29.    pinMode(12,OUTPUT);
30.    pinMode(2,OUTPUT);
31.    pinMode(3,OUTPUT);
32.    // initialize serial communication at 9600 bits per second:
33.    Serial.begin(9600);
34.    while (!Serial) {
35.      ; // wait for serial port to connect. Needed for native USB, on
 LEONARDO, MICRO, YUN, and other 32u4 based boards.
36.    }
```

```
37.
38.    if (!lox.begin()) {
39.      Serial.println(F("Failed to boot VL53L0X"));
40.      while(1);
41.    }
42.
43.    // Now set up two tasks to run independently.
44.    xTaskCreate(
45.      Beep
46.      ,  "Beep"   // A name just for humans
47.      ,  128  // This stack size can be checked & adjusted by reading
 the Stack Highwater
48.      ,  NULL
49.      ,  2  // Priority, with 3 (configMAX_PRIORITIES - 1) being the
highest, and 0 being the lowest.
50.      ,  NULL );
51.
52.    xTaskCreate(
53.      TaskDistanseRead
54.      ,  "AnalogRead"
55.      ,  128  // Stack size
56.      ,  NULL
57.      ,  1  // Priority
58.      ,  NULL );
59.    // Now the task scheduler, which takes over control of scheduling
 individual tasks, is automatically started.
60.
61.  }
62.
63.  void loop()
64.  {
65.    digitalWrite(12,digitalRead(8));//Enable milinmeter wave based on
 hall switch.
66.    while(Serial.available(){
67.      char inchar = Serial.read();
68.      if(inchar == 0xF4) pos_x = Serial.parseInt();
69.      if(inchar == 0xF5) pos_y = Serial.parseInt();
70.    }
71.    if(pos_x*pos_x+pos_y*pos_y<1000){
72.      if(x<0){
73.        digitalWrite(2,HIGH);
74.        digitalWrite(3,LOW);
```

```
75.       }
76.       else{
77.         digitalWrite(2,LOW);
78.         digitalWrite(3,HIGH);
79.       }
80.     }
81.     else{
82.       digitalWrite(2,LOW);
83.       digitalWrite(3,LOW);
84.     }
85.   }
86.
87.   /*--------------------------------------------------*/
88.   /*---------------------- Tasks ---------------------*/
89.   /*--------------------------------------------------*/
90.
91.   void Beep(void *pvParameters)  // This is a task.
92.   {
93.     (void) pvParameters;
94.     // initialize digital LED_BUILTIN on pin 13 as an output.
95.     pinMode(Buzzer_pin, OUTPUT);
96.
97.     for (;;) // A Task shall never return or exit.
98.     {
99.       if(close_to){
100.        digitalWrite(Buzzer_pin,HIGH);
101.        vTaskDelay(10);// one tick delay (15ms) in between
102.        digitalWrite(Buzzer_pin,LOW);
103.        vTaskDelay(Beep_Duration);// one tick delay (15ms) in between
104.      }
105.
106.    }
107.  }
108.
109.  void Beep(void *pvParameters)  // This is a task.
110.  {
111.    (void) pvParameters;
112.    // initialize digital LED_BUILTIN on pin 13 as an output.
113.    pinMode(Buzzer_pin, OUTPUT);
114.
115.    for (;;) // A Task shall never return or exit.
```

```
116.   {
117.     if(close_to){
118.       digitalWrite(Buzzer_pin,HIGH);
119.       vTaskDelay(10);// one tick delay (15ms) in between
120.       digitalWrite(Buzzer_pin,LOW);
121.       vTaskDelay(Beep_Duration);// one tick delay (15ms) in between

122.     }
123.
124.   }
125. }
126.
127. void TaskDistanseRead(void *pvParameters)  // This is a task.
128. {
129.   (void) pvParameters;
130.
131. /*
132.   AnalogReadSerial
133.   Reads an analog input on pin 0, prints the result to the serial m
onitor.
134.   Graphical representation is available using serial plotter (Tools
 > Serial Plotter menu)
135.   Attach the center pin of a potentiometer to pin A0, and the outsi
de pins to +5V and ground.
136.
137.   This example code is in the public domain.
138. */
139.
140.   for (;;)
141.   {
142.     // read the input on analog pin 0:
143.     lox.rangingTest(&measure, false); // pass in 'true' to get debu
g data printout!
144.
145.     if (measure.RangeStatus != 4) {  // phase failures have incorre
ct data
146.       int Measure_Result = Serial.println(measure.RangeMilliMeter);
147.       if(Measure_Result<1000){
148.         close_to = true;
149.         if(Measure_Result>500) Beep_Duration = 100;
150.         else if(Measure_Result>300) Beep_Duration = 50;
151.         else Beep_Duration = 20;
```

```
      }
    }
// The buzzer will beep when the distance is less than 1m.
// The buzzer will beep faster when the distance is less than 0.5m.
// The buzzer will beep the fastest when the distance is less than
0.3m.
// The buzzer will stop when the distance is more than 1m.
// The buzzer will stop when the hall switch is off.
// The buzzer will stop when the watch is on the table.
// The buzzer will stop when the watch is on the user's hand.

    vTaskDelay(20);  // one tick delay (15ms) in between
  }
}
// end of loop
// end of code
```